

1 **Flagellin FLiC Enhances Resistance of Upland Cotton to *Verticillium*** 2 ***dahliae***

3 Heng Zhou¹, Yijing Xie¹, Yi Wang¹, Heqin Zhu^{2*}, Canming Tang^{1*}

4 1 State Key Laboratory of Crop Genetics and Germplasm Enhancement, College of
5 Agriculture, Nanjing Agricultural University, 210095 Nanjing, China.

6 2 State Key Laboratory of Cotton Biology, Institute of Cotton Research of Chinese
7 Academy of Agricultural Sciences, Anyang, 455000 Henan, China.

8 *Author for correspondence: Heqin Zhu, Email: heqinanyang@163.com.

9 Canming Tang, Email: tangcm@njau.edu.cn.

10 **Abstract:**

11 The mechanism by which flagellin induces an immune response in plants is still unclear.
12 The purpose of this study is to reveal the effect and mechanism of flagellin in inducing
13 plants to produce an immune response to increase the resistance to *Verticillium dahliae*
14 (VD). The full-length flagellin gene C (FliC) was cloned from an endophytic bacteria
15 (*Pseudomonas*) in the root of upland cotton cultivar Zhongmiansuo 41. The FliC protein
16 purified in vitro has 47.50% and 32.42% biocontrol effects on resistant and susceptible
17 cotton cultivars, respectively. FLiC can induce allergic reactions in tobacco leaf cells and
18 immune responses in cotton plants. Smearing FLiC to cotton and performing RNA-seq
19 analysis, it is significantly enriched in the activity of positive ion transporters such as
20 potassium ions and calcium ions (Ca²⁺), diterpenoid biosynthesis, phenylpropane
21 biosynthesis and other disease-resistant metabolic pathways. FLiC inhibits the expression
22 of calcium antiporter activity gene (*GhCAA*) to accelerate intracellular Ca²⁺ influx and
23 stimulate the increase of intracellular hydrogen peroxide (H₂O₂) and nitric oxide (NO)
24 content. The coordinated regulation of Ca²⁺, H₂O₂ and NO enhances disease resistance. The
25 resistance of transgenic *FLiC* gene Arabidopsis to VD was significantly improved. The
26 *FLiC* gene can be used as an anti-VD gene and as a regulator to improve resistance to VD.

27

28 **Key words:** Flagellin, immune response, *Verticillium dahliae*, Ca²⁺, RNA-seq

29

30 **Abbreviations:** 2-DDG: 2-deoxy-D-glucose; AOPP: α -aminoxyacetic acid- β
31 -phenylpropionic acid; Ca²⁺: calcium ions; H₂O₂: hydrogen peroxide; NO: nitric oxide;
32 *GhCAA*: calcium antiporter activity gene; PTI: pattern triggered immunity; ETI: effector

33 triggered immunity; ROS: reactive oxygen species; SA: Salicylic acid; JA: Jasmonic acid;
34 IPTG: isopropyl- β -D thiogalactopyranoside; PMSF: phenylmethanesulphonyl fluoride;
35 PVP: polyvinyl pyrrolidone; CHI: chitinase; GLU: glucanase; PAL: Phenylalanine
36 ammonia lyase; PPO: polyphenoloxidase; POD: Peroxidase; CAT: catalase; qRT-PCR:
37 quantitative reverse transcriptase-PCR; DAB: 3,3'-diaminobenzidine; CAT: catalase;
38 C-PTIO: carboxy-2-phenyl-4,4,5,5-tetramethylimidazoline-3-oxide-1-oxyl); L-NAME:
39 nitro-L-arginine methyl ester; EGTA: ethylene glycol-bis(2-aminoethyl
40 ether)-N,N,N',N'-tetraacetic acid; VD: *Verticillium dahliae*; *PR1*: disease-related protein 1;
41 *LOX*: lipoxygenase; *VSP*: vegetative storage protein; *GPX7*: glutathione peroxidase;
42 *GSTU3*: glutathione sulfur transfer Enzyme gene; *FLiC*: full-length flagellin gene C.

43

44 **Introduction:**

45 Immune response is closely related to the disease resistance of plants. Plants mainly
46 rely on two levels of defense pathways to resist infection by pathogens: pathogenic
47 microorganisms pattern triggered immunity (PTI) (Nürnberger and Brunner, 2002) and
48 pathogens secreted effector triggered immunity (ETI) (Thomma et al., 2011; Naveed et al.,
49 2020). The defense response is realized by mutual recognition and interaction between the
50 recognition receptors of plants and the elicitors secreted by pathogenic microorganisms.
51 Through the transmission and transduction of a series of signals to activate the immune
52 defense response in the plant, and finally make the plant obtain systemic disease resistance
53 (Jennings et al., 2001; Bouizgarne et al., 2006; Jones et al., 2006; Kumar et al., 2020). The
54 early defense reactions of plants mainly include the production of early disease resistance
55 signals such as allergic reactions, reactive oxygen species (ROS) outbreaks, and NO
56 accumulation. These stimulus signals are converted from extracellular to intracellular
57 signals and amplified by a cascade reaction to induce downstream defense reactions. These
58 reactions always occur first around the infected tissue and gradually spread to the
59 surrounding uninfected tissues. In the end, the immune system of the entire plant is
60 activated to defend against the infection of various pathogens (Dixon et al.,1994; Ebel et
61 al.,1998; Yano et al.,1998; Durrant et al., 2004; Buxdorf et al., 2013; Holmes et al., 2021).

62 Flagellin can induce immune responses in rice, algae and kelp but the mechanism is
63 unclear (Takai et al., 2008; Wang, 2012; Wang et al., 2013). The flagellin Flg22 cloned
64 from *Pseudomonas syringae* is a 22-amino acid peptide conserved at the N-terminus, which
65 acts as an active site for elicitor to induce immune responses in higher plants (Felix et al.,
66 1999). After being induced by flagellin, plants will produce a series of defense responses,
67 including ethylene (ETH) production, callose deposition, ROS burst, defense gene
68 expression and growth inhibition (Asai et al., 2002; Zipfel et al., 2004). Flg22 is mainly
69 based on salicylic acid (SA) signal transduction pathway, and also related to jasmonic acid
70 (JA) or ethylene signal transduction pathway (Gómez-Gómez et al., 2000; Yuan et al.,
71 2020). Activated SA and JA signaling pathways have an effect on the ROS burst and
72 callose deposition triggered by Flg22 (Yi et al., 2014). The effect and mechanism of
73 exogenous protein and Flg22 in inducing the immune response of upland cotton have not
74 been studied.

75 *Verticillium wilt* of cotton is mainly a soil-borne vascular disease caused by VD. It
76 seriously affects cotton yield and fiber quality and lacks effective control measures. The
77 effect and mechanism of exogenous protein inducing immune response in cotton to
78 increase resistance to VD has not been reported. In this study, a full-length flagellin gene
79 *FliC* was cloned from cotton endophytic bacteria (*Pseudomonas*). The purpose of this study
80 was to study the effect and mechanism of this protein in inducing cotton immune response
81 and improving resistance to VD.

82 **Materials and Methods**

83 **Microbial strains and cotton cultivar**

84 VD were generously provided by the Institute of Plant Protection, Jiansu Academy of
85 Agriculture Sciences. Hygromycin B-resistant GFP-labelled VD was provided by Hu (2012)
86 and maintained on potato dextrose agar (PDA) at 25°C. For the inoculation assay, conidia
87 from 10-day-old PDA plates inoculated with the V1070 were washed once with sterile
88 water and diluted to a concentration of 10^7 conidia mL⁻¹. The expression vector Pgex-4T-2
89 and *Escherichia coli* expression competent cell *E.coli* BL21 (DE3) was purchased from
90 Beijing Kinco Xinye Biotechnology Co., Ltd. The tested tobacco variety was *Nicotiana*

91 *tabacum* cv. Xanthi NN, which was cultivated in a greenhouse at 25°C to the 7-8 leaf stage.
92 The tested cotton varieties were the VD-susceptible variety Jimian 11 and the
93 disease-resistant cotton variety Zhongzhimian 2.

94

95 **Construction of *FliC* gene expression vector**

96 Using P_{gex}-4T-2 as an expression vector and designing a pair of specific primers
97 based on the *FliC* gene sequence:

98 *FliC*-BamHI-F: 5'- CGCGGATCCATGGCCTTGACCGTCAACAC-3'

99 *FliC*-EcoRI-R: 5'- CCGGAATTCTTAGCGCAGCAGGCTCAGAAC-3'

100 PCR reaction system: *FliC*-BamHI-F: 2.0 μL; *FliC*-EcoRI-R: 2.0 μL; Gold Mix (green):
101 45.0 μL; Plasmid: 1.0 μL with a total volume of 50.0 μL. PCR amplification conditions:
102 pre-denaturation at 98°C for 2 min; denaturation at 98°C for 10 s, annealing at 62°C for 30
103 s, extension at 72°C for 10 s, 35 cycles; extension at 72°C for 2 min. Finally, perform
104 agarose gel electrophoresis detection (1.5% agarose, 120V, 20 min). Use TAKARA gel
105 recovery kit to recover the amplified products. The recovered product and P_{gex}-4T-2 were
106 digested at 37°C for 5 hours. Use T4 ligase to ligate overnight at 16°C. PCR detection
107 conditions of bacterial solution: pre-denaturation at 98°C for 2 min; denaturation at 98°C
108 for 10 s, annealing at 55°C for 30 s, extension at 72°C for 20 s, 35 cycles; extension at
109 72°C for 1 min. The recombinant expression plasmid *FliC*- P_{gex}-4T-2 verified by PCR
110 amplification, restriction enzyme digestion and sequencing was transformed into competent
111 cells of E.coli BL21(DE3) for prokaryotic expression.

112

113 **Induced expression of recombinant protein FLiC**

114 Pick a single colony of the positive strain, inoculate 5 mL in a fresh LB liquid medium
115 containing 50 mg/L ampicillin, and culture with shaking at 37°C until the OD₆₀₀ is 0.6-0.8.
116 Add isopropyl-β-D thiogalactopyranoside (IPTG) with a final concentration of 0.5 mM,
117 and continue shaking culture at 150 rpm for 5 hours at 28°C. Polyacrylamide gel
118 electrophoresis (SDS-PAGE) detection, with non-induced bacterial liquid and BL21 (DE3)
119 bacterial liquid as controls.

120

121 **FLiC protein allergic reaction test**

122 Using 5-6 true leaf tobacco seedlings as experimental materials, 50 μL (100 $\mu\text{g}/\text{mL}$) of
123 purified protein was injected into the mesophyll from the back of the leaf, GST as controls,
124 and each treatment was repeated 3 times(Felix et al.,1999; Gómez-Gómez et al., 2000)。

125 **Detection of disease resistance of FLiC to cotton cultivars**

126 Four-leaf stage seedlings of uniformly growing disease-resistant cotton varieties
127 (Zhongzhimian 2) and susceptible varieties (Jimian 11) were selected, and FLiC at a
128 concentration of 50 $\mu\text{g}/\text{mL}$ was uniformly smeared to treat cotton seedling leaves. Water is
129 used as a control. After treatment for 2 days, inoculate the pathogenic spore suspension (2
130 $\times 10^7$ cfu/mL). The method of inoculation of the pathogen is as follows: remove the cotton
131 seedlings, soak the roots in the pathogen spore suspension for 20 minutes, inoculate 15
132 strains of each cotton cultivar with sterile water as the control. 15 days after inoculation,
133 the incidence of cotton was counted. At the same time, observe the infection of disease
134 bacteria in cotton roots, stems and leaves during this period under a microscope. The
135 condition was investigated 30 days after inoculation, and all experiments were repeated 3
136 times.

137

138 **Lignin detection**

139 According to Pomar's method, Wiesner reagent is used to detect the content of lignin
140 (Pomar et al., 2002). Each treatment is repeated three times.

141 **callose detection**

142 Refer to Millet's method for corpus callosum detection (Millet et al., 2010). The
143 quantification of callose is calculated by Image J software. Each treatment was repeated
144 three times.

145

146 **Biomass detection of VD**

147 Cut two cotyledons from cotton of different treatment groups in a sterile environment,

148 weigh and add 2 mL of sterile water for grinding. After grinding into a homogenate, it is
149 diluted according to the method of gradient dilution. 100 μ L of diluents of different
150 concentrations were spread on the red bengal resistant medium containing 50 μ g/mL
151 hygromycin and 50 μ g/mL streptomycin, and then placed in a 28°C constant temperature
152 incubator and cultured upside down for 2 days. Count the number of colonies in each petri
153 dish and calculate the content of VD per gram of leaf. All experiments were repeated three
154 times (Wang, 2014) .

155

156 **Chitinase(CHI) and glucanase(GLU) detection**

157 Enzyme extracts from cotyledon were prepared in 0.2 M boric acid-borax buffer, pH
158 7.6 with 0.1% (v/v) β -mercaptoethanol, 0.57 mM phenylmethanesulphonyl fluoride
159 (PMSF) and 1% (w/v) polyvinyl pyrrolidone (PVP) and 50 mM potassium acetate buffer
160 (pH 5.0) for CHI and GLU, respectively. The homogenate was centrifuged at 12,000 \times g for
161 20 min at 4°C and the supernatant served as enzyme source. CHI activity was measured
162 according to the protocol described by Emani et al (2003) using 4-methylumbelliferyl- β -
163 -D-N, N''-triacetylchitotrioside [4-MU- β -(GlucNAc)₃] (Sigma, St. Louis, MO, USA) as
164 the substrate. Enzyme extract were further diluted (16-fold) with 0.1 M citrate buffer, pH
165 3.0 prior to the enzyme assay. One hundred microlitres of diluted protein extract were
166 mixed with 25 μ L of substrate (250 μ M) and incubated at 30°C for 1 h. The reaction was
167 terminated with 1 mL of 0.2 M sodium carbonate and fluorescence was measured using a
168 DyNA Quant™ 200 fluorometer (Hoefer). The endochitinase activity is presented as pmole
169 4-MU/h/mg protein. Each assay was carried out in three replicates.

170 The GLU assay was performed using the method of Abeles and Forrence (1970).
171 Laminarin was used as the substrate and dinitrosalicylic reagent was used to measure the
172 reducing sugars produced in the enzymatic reaction. 0.5 mL enzyme extract was routinely
173 added to 0.5 mL of 2% (w/v) laminarin in water and incubated at 50°C for 1 or 2 h. The
174 laminarin was dissolved by heating the 2% solution briefly in a boiling water bath before
175 use. The reaction was stopped by adding 3 mL of the dinitrosalicylic reagent and heating
176 the tubes for 5 min at 100°C. The tubes were then cooled to 25°C, the contents were diluted

177 1:10 with water, and the optical density was read at 500 nm. The enzyme activity is
178 expressed as glucose equivalents, mg/h/mg protein. Each assay was carried out in three
179 replicates.

180 **Phenylalanine ammonia lyase (PAL) and polyphenoloxidase (PPO)** 181 **detection**

182 Enzyme extracts from cotyledon were prepared in 0.1 M sodium borate buffer, pH 7.0
183 containing 0.1 g insoluble PVP and 0.1M sodium phosphate buffer (pH 6.5) for PAL assays
184 and PPO, respectively. The homogenate was centrifuged at 12,000×g for 20 min at 4°C
185 and the supernatant served as enzyme source. Samples containing 0.4 mL of enzyme
186 extract were incubated with 0.5 mL of 0.1 M borate buffer, pH 8.8, and 0.5 mL of 12 mM
187 L-phenylalanine in the same buffer for 30 min at 30°C. PAL activity was determined as the
188 rate of conversion of L-phenylalanine to trans-cinnamic acid at 290 nm as described by
189 Dickerson et al (1984) and was expressed as nmoles of cinnamic acid unit min/mg protein.

190 The method for determining the activity of PPO is slightly modified with reference to
191 the method of Ali et al (2006). Add 1 mL of 0.05 mol/L phosphate buffer (pH 5.5) to the
192 0.2g leaves uniformly ground with liquid nitrogen, shake and mix, and centrifuge at 4° C,
193 12000rpm for 15min. Take 0.5 mL of the supernatant enzyme solution and add 1.0 mL of
194 0.1 M catechol solution and 1.5 mL of 0.05 mol/L pH 5.5 phosphate buffer, the total
195 volume is 3 mL. After mixing uniformly, measure the absorbance at 398 nm every 2
196 minutes, and use 0.05 mol/L (pH 5.5) phosphate buffer as a control. Take $\Delta A_{398}/\Delta t$
197 =0.01/min to express an enzyme activity unit (U). Each assay was carried out in three
198 replicates

199

200 **Peroxidase (POD) and catalase (CAT) detection**

201 Enzyme extracts from cotyledon were prepared in 50 mM Tris-HCl buffer, pH 7.0.
202 The extract was centrifuged at 12 000 g for 20 min at 4°C. The supernatant was passed
203 through a Sephadex G-25 column and fractions containing enzyme were pooled and used
204 as enzyme source for the assay of catalase and POD by Sudhakar et al (2001).
205 The determination of peroxidase activity is slightly modified according to the method of
206 Dong et al (2003). Add 0.2g of the leaves uniformly ground with liquid nitrogen to 1mL of

207 0.1M pH 5.5 phosphate buffer, shake and mix well, and centrifuge at 4° C at 12000rpm for
208 15min. Take 0.1mL of the supernatant enzyme solution and add 2.9mL of 0.05mol/L
209 phosphate buffer, 1mL of 0.05mol/L guaiacol and 1mL of 2% H₂O₂. Measure the
210 absorbance value at 470 nm immediately after mixing, and the change of A₄₇₀ by 0.01 per
211 minute is 1 peroxidase activity unit (u). Each assay was carried out in three replicates.

212 CAT activity was measured using the method of Plazek and Zur (2003) with a
213 modification. CAT activity was assayed in reaction mixture (3 cm³ final volume) composed
214 of 50 mM Tris-HCl buffer pH 7.0 to which 30% (w/v) H₂O₂ was added to reach an
215 absorbance value in the range 0.520 - 0.550 (λ =240 nm). The reaction was started after
216 adding 200 μ L of crude extracts to the reaction mixture. CAT activity was measured as a
217 decrease in absorbance at 240 nm as a consequence of H₂O₂ consumption. Activity of the
218 enzyme was expressed as mmol H₂O₂ decomposed per minute per milligram of protein.
219 Each assay was carried out in three replicates.

220 **RNA extraction and gene expression analysis by quantitative reverse** 221 **transcriptase-PCR (qRT-PCR)**

222 Leaves were collected and transcript analysis was conducted at different time points as
223 indicated in the figures. Analyses were performed by quantitative qRT-PCR. RNA
224 extraction and gene expression analysis were performed as previously described by Ren et
225 al (2013) with slight modifications. Total RNA was extracted using an RNA Isolation Kit
226 (Omega Bio-Tek) according to the manufacturer's instructions. First-strand complementary
227 DNA was synthesized from total RNA using a PrimeScriptTM RT reagent kit with gDNA
228 Eraser (Takara, China). Then, 5 μ L of 1:10 diluted cDNA samples was used as the
229 qRT-PCR template with 0.5 μ M gene-specific primers and 10 μ L SYBR Premix Ex Taq II
230 (Takara, China) in a total volume of 20 μ L. Experiments were performed in a Realplex2
231 Systems (Eppendorf, Germany) with the following thermal cycling profile: 95°C for 10 min,
232 followed by 40 cycles of 95°C for 30 s, 55°C for 30 s, and 72°C for 30 s. Each real-time
233 assay was tested in a dissociation protocol to ensure that each amplicon was a single
234 product. Sequences of cotton defense gene primers were used for RT-qPCR (Supplemental
235 Table S1). Relative gene expression of genes was calculated by the threshold cycle $2^{-\Delta\Delta CT}$

236 method by Livak and Schmittgen (2001) from three biological replicates and three
 237 technical replicates. For each gene, the mean fold-change \pm SD in transcript accumulation
 238 within treated leaves relative to the control (set at 1.0) was calculated from three biological
 239 replicates.

240 Supplemental Table S1 Primer sets used for quantitative real-time PCR

Primer	Sequence	Ref	Gene
<i>CHI</i>	ACCAAGCTACTCGCAAGAGG' CGGAAGCGCAGTAAGATGA	CD485880	Pathogen induced class1 chitinase
<i>GLU</i>	CATTGATATGACCTTGATCG GTGAGATATCCCTTGGATTG	CD486342	Pathogen induced glucanase
<i>HMG</i>	GATTTGAAGTTGTATTTGGAG GAAATCAGTTTGAAGGAAA	CD486522	Pathogen induced HMG CoA reductase
<i>LOX</i>	AGTCGTCGGTTCATGCCTGAGAAA ATTCCCAGGAGTGTCTGCAGTTGA	Han, 2014	Pathogen induced lipoxygenase
<i>POD4</i>	TTTGCTGTGCCATGGTGAAGATG CAATCAGTTGACCACCCTGCAGTT	AF155124	Pathogen induced peroxidase
<i>PR1</i>	TGCCCAAGACTCACAACAAG GGCCTTCTCATTAACCCACA	Han, 2014	Putative PR1
<i>ERF5</i>	GCTCAAGCCGGTTTAAATATGGGT TTCACCACATGTACAAGGTCCCAC	Han, 2014	Bacterial-induced ERF5 gene
<i>CDN1</i>	GCCAACTTGTGGTTATGCCATGCT TGCTGAGCAATCGTCTTCTCTCCT	Han, 2014	Terpenoid aldehydes and cadalene derivitives
<i>PR10</i>	ATGATTGAAGGTCGGCCTTTAGGG CAGCTGCCACAACTGGTTCTCAT	Han, 2014	Putative PR10
<i>MAPK2</i>	TTACAATCTTATTCCACACACGC TCCCTATTTATAGAAAACCTCCC	DQ132852.1	Mitogen-activated protein kinase
<i>MAPK6</i>	GGACACTGAGATGGCGGAGC ACCAATGGGCATAATAGGAG	JF727638.1	Mitogen-activated protein kinase
<i>MAPK7</i>	CAGAGCAAATATGCCGTATG TTACAATCTTATTCCACACACGC	FJ966888.1	Mitogen-activated protein kinase
<i>MAPK16</i>	GTGTTGTTTGTTCAGCGTATG CGTAGGAGCCTGAGAAGTTTA	FJ966889.1	Mitogen-activated protein kinase

<i>WRKY2</i>	TTCTTCCCATAATACCATCC CTCGCATAAACTGTTAGCATC	DQ864758.1	Transcription factor
<i>WRKY3</i>	GGGACGAAAGTTGTCAAAGGGAA TCGTGTTGCTGTTTCGGTTG	FJ966887.1	Transcription factor
<i>WRKY4</i>	ATTGATAACAACCTTACGAGGGC TTGAGGAGCAAGGAAGGATT	JQ081265.1	Transcription factor
<i>WRKY5</i>	GCAAAGGGAACCGAGATT ATCGGGTAGGGATGCTTG	JQ081266.1	Transcription factor
<i>WRKY6</i>	AAGCCAATCAAGGGTTCTCC GTTCTTCCAAGCACCTCTCT	JQ081267.1	Transcription factor
<i>18S rRNA</i>	CCATAAACGATGCCGACCAG AGCCTTGCGACCATACTCCC	HQ658359.1	18S ribosomal RNA gene

241

242 **Measurement of cytosolic Ca²⁺ concentration**

243 To measure cytosolic calcium concentration, epidermal strips of four-week-old cotton
244 leaves were loaded with the Ca²⁺-sensitive fluorescent dye 1-[2-amino-5-(2,
245 7-dichloro-6-hydroxy-3-oxo-9-xanthenyl) phenoxy]-2-(2-amino-5-methylphenoxy) ethane-
246 N, N, N', N' -tetraacetic acid, pentaacetoxymethyl ester (Fluo-3/AM) (Molecular Probes,
247 Eugene, OR, USA), which was observed with the laser-scanning confocal microscopy
248 (LSCM) according to the method described by Chen et al (2004). The cotton epidermal
249 strips were incubated in 10 μM Fluo-3 AM loading buffer (10 mM MES-Tris, pH 6.1) at
250 4°C for 2 h in darkness. After incubation at 4°C for 2 h in the dark, the epidermal strips
251 were washed twice with anisotonic solution and incubated at 25°C for 1 h in the dark. The
252 epidermal peels loaded with Fluo-3/AM were exposed to FLiC (100 μg/mL) and distilled
253 water (control) for 12 min. Fluorescent probes were excited with a 488 nm laser, and the
254 emission fluorescence was filtered by a 515 nm filter to eliminate the autofluorescence of
255 the epidermal strips. Images were recorded every 20 s. Images were analyzed using Leica
256 IMAGE software. All of the experiments were repeated three times, and the Ca²⁺ fluxes of
257 6 horizons of epidermal cells were measured in each treatment at each time. Pictures were
258 taken by scanning the field of view three times each 20 s; then, the fluorescence intensities

259 of these pictures were measured by fluorescence microscopy after establishing a stable
260 baseline.

261 **H₂O₂ detection and quantification**

262 Detection of H₂O₂ was also performed based on the method described by Kumar et al
263 (2009) with slight modifications. The leaves were harvested and placed in a solution
264 containing 1 mg mL⁻¹ 3, 3' -diaminobenzidine (DAB) (pH 3.8) for 8 h under light at 25°C.
265 The leaves were boiled in ethanol (96%, v/v) for 10 min and then stored in 96% ethanol.
266 H₂O₂ production was visualized as a reddish-brown coloration of the leave. The
267 concentration of H₂O₂ in plant leaves was measured by monitoring the A₄₁₅ of the
268 titanium-peroxide complex following the method described by Brennan and Frenkel (1977).
269 Absorbance values were calibrated to a standard curve generated with known
270 concentrations of H₂O₂. The total H₂O₂ content was recalculated for 1 g of fresh weight of
271 plant leaves.

272 **NO detection and quantification**

273 The levels of NO in cotton leaves were determined with the Griess reagent kit
274 (Beyotime Institute Biotech) described by Li et al (2010) with slight modifications. The
275 optical density at 550 nm of the reaction product was measured with a UV mini-1240
276 spectrophotometer (Shimadzu, Japan). The production of NO (mol g⁻¹ of fresh weight) was
277 calculated with a formula supplied in the kit. There were three replicates in each treatment.
278 Nitric oxide in cotton epidermal cell was visualized using the specific NO probes 3-Amino,
279 4-aminomethyl-2', 7' -difluorescein diacetate 4, 5-diaminofluorescein diacetate (DAF-FM
280 DA, Sigma-Aldrich) (Sun et al., 2012) using the method described by Bright et al(2006) .
281 FLiC or inhibitors as indicated the figures or figures legends, and then incubated in
282 MES-KCl buffer (10 mM MES, 5 mM KCl, 50 µM CaCl₂, pH 6.15) and DAF-FM DA at a
283 final concentration of 10 M for 30 min in the dark at 25°C, followed by washing twice in
284 the same MES-KCl buffer for 15 min each. All images were visualized using CLSM
285 (excitation 488 nm, emission 515 nm). Images acquired were analyzed using Leica IMAGE
286 software. All treatment s were repeated three times. The data are presented as the average

287 fluorescence intensity.

288

289 **Transcriptome Differential Gene Significance Screening Conditions**

290

291 Define the genes with $|\log_2FC| \geq 1$ and P-value ≤ 0.05 , and screen them as
292 significantly differentially expressed genes. The significant enrichment conditions of
293 metabolic pathways are used to calculate the P-value by the hypergeometric distribution
294 method (the standard for significant enrichment is P-value < 0.05).

295

296 **Primer design for qRT-PCR verification of transcriptome results**

297 According to the results of RNA-seq sequencing, 12 genes were randomly selected to
298 design gene-specific primers by NCBI and verified by qRT-PCR (Supplemental Table S2).

299 The relevant primer designs are as follows:

300

301 Supplemental Table S2 Specific primer sequences of qRT-PCR related genes

Gene name	Primer sequence (5'→3')	
<i>GH_D07G1376</i>	F:GTTGGTCACGACCGAGGAG;	R:AGCCCTCTTGAAATTAGCCCC
<i>GH_D09G0121</i>	F:GGTCTTTATTTATTGTGACAGGTGG;	R:GCTGGTGGAAATGGAAAACCG
<i>GH_A11G1348</i>	F:ACAGGCAGCATACTAGGTGG;	R:TCCTCTAGCTCTTGGCCCTT
<i>GH_A02G0915</i>	F:GCAGTCGACATCACAAAACCTC;	R:GGCCTCCACTACGGACTCTT
<i>GH_A08G0063</i>	F:ACCTATACCTGGCGAGTTTTG;	R:AATCCACCCAACCACAACACA
<i>GH_D08G0067</i>	F:ACCTATACCTGGCGAGTTTTG;	R:AATCCACCCAACCACAACACA
<i>GH_A09G1367</i>	F:CCGCTGGAGGTAGGAAAAGG;	R:CGATTTCTTCGCCCGGTTTC
<i>GH_D03G1291</i>	F:AACACTGATGCAGAAGGTAGG;	R:TGTTGCCAGGTCAAGATGTCTA
<i>GH_A13G0836</i>	F:CCATCTTCTCCCTCTTGGCA;	R:AAGCTGGGTTACAAGGCAAG
<i>GH_D01G0069</i>	F:GTGTCTGGCTTTGTCTGCTGTA;	R:CTTCGATCGATGCAAACGACA
<i>GH_D10G0737</i>	F:ACTCCTTGTTACCAGCCGAAA;	R:CTCTGTGAAGACAAGCTGCC
<i>GH_A10G0542</i>	F:AGTTCGTCCAAGCGAAGGAG;	R:TCTTCAACCCCGCTTTACC
<i>ubiquitin</i>	F:GAGTCTTCGGACACCATTG;	R:CTTGACCTTCTTCTTCTTGTGC

302

303 **Statistical analysis**

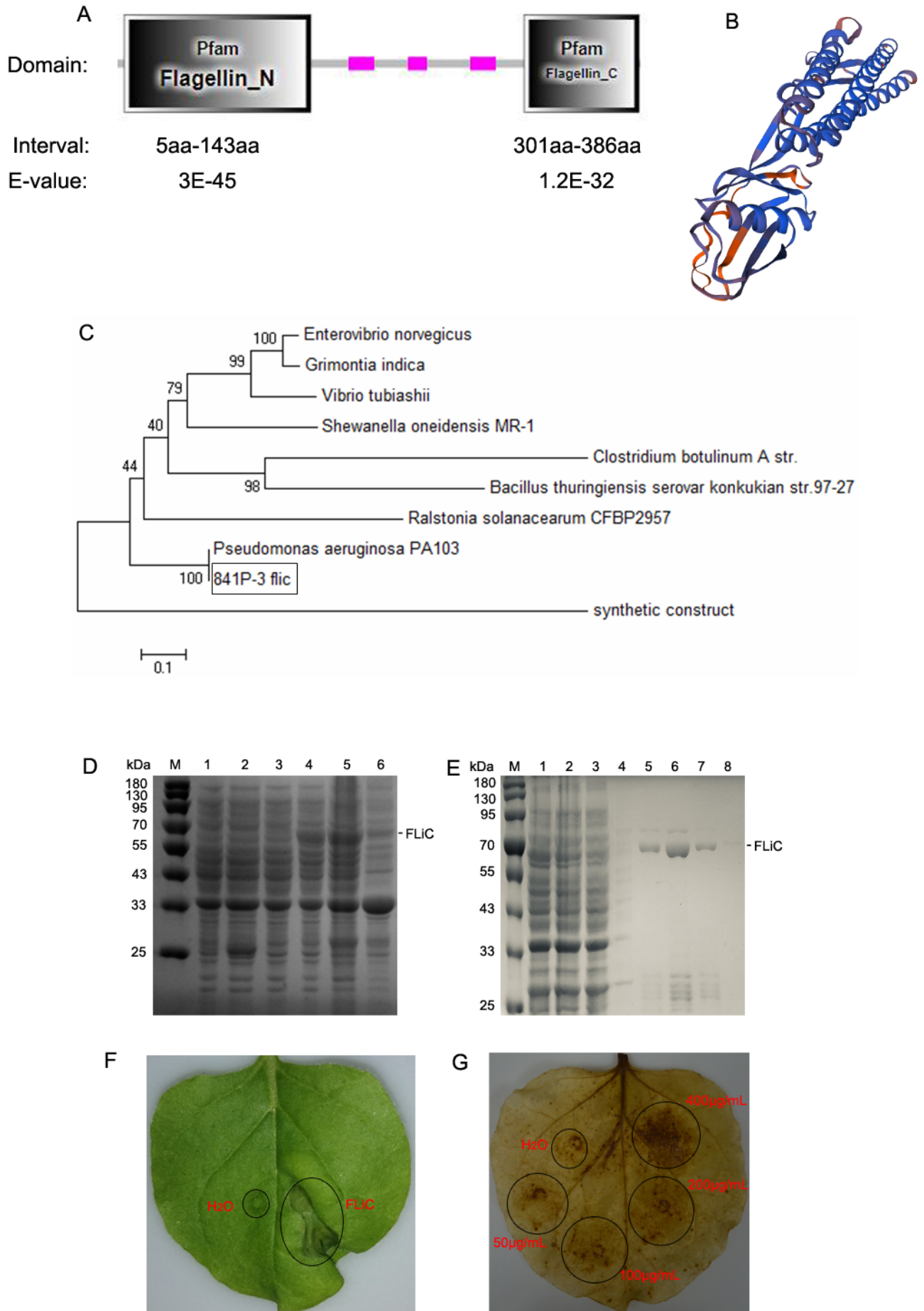
304 All experiments and data provided in this paper were repeated at least three times. The
305 resulting data were subjected to an analysis of variance using GraphPad Prism software
306 version 4.0 and SPSS 19.0 software (SPSS Inc.). Student's unpaired t test and Student -

307 Newman - Keuls (S - N - K) test ($P < 0.05$) were used to determine the significance of the
308 differences observed between the samples.

309 **Results**

310 **The structure and allergic reaction of flagellin FLiC**

311 FLiC protein is flagellin and has two functional domains (Figure 1A). It has
312 three-dimensional structure (Fig. 1B). The homology with *Pseudomonas aeruginosa* PA103
313 is 100% (Figure 1C). The recombinant plasmid was transformed into *E. coli* BL21 (DE3)
314 strain, and induced by Isopropyl- β -D-thiogalactopyranoside (IPTG) (0.5 mM) at 28°C for
315 5 h. The purified FLiC protein was 66 kDa (Figure 1, D and E). FLiC protein induces
316 hypersensitive reaction and reactive oxygen species in tobacco leaves (Figure 1, F and G).



318 **Figure 1** The structure and allergic reaction of flagellin FLiC
319 A, two functional domains of FLiC protein; B, three-dimensional structure diagram of FLiC protein;
320 C, evolutionary tree of FLiC protein; D: Expression of FLiC recombinant protein in *E. coli* at 28°C;
321 M: protein marker; 1: control containing empty vector; 2: empty vector with the addition of inducer
322 (0.5 mM IPTG); 3: Whole bacteria added with inducer (0 mM IPTG); 4: Whole bacteria added with
323 inducer (0.5 mM IPTG); 5: The supernatant part after the bacterial cell is broken; 6: The part that
324 settles after the bacterial cell is broken. E: purified FLiC protein; M: protein marker; 1: cell lysate;
325 2: flow through; 3: wash1; 4: wash2; 5: elution1; 6: elution2; 7: elution3; 8: elution4. F:
326 hypersensitive reaction(HR) of FLiC on tobacco; G: reactive oxygen species (ROS) generated
327 after treatment with different FLiC protein concentration,
328

329 **FLiC induces resistance of cotton to VD**

330 After smearing Jimian 11 and Zhongzhimian 2 with FLiC protein, the amount of VD
331 in roots, stems and leaves was significantly lower than that in the control group, indicating
332 that FLiC can induce resistance to the infection of VD (Figure 2). The incidence of resistant
333 varieties was lower than that of susceptible varieties. After 30 days of FLiC treatment, the
334 disease index of resistant varieties was lower than that of susceptible varieties. The relative
335 biocontrol effects of FLiC on resistant and susceptible cotton varieties were 47.50% and
336 32.42% respectively (Table 1). Therefore, FLiC can not only induce systemic disease
337 resistance in cotton, but the induction effect of resistant varieties is stronger than that of
338 susceptible varieties.

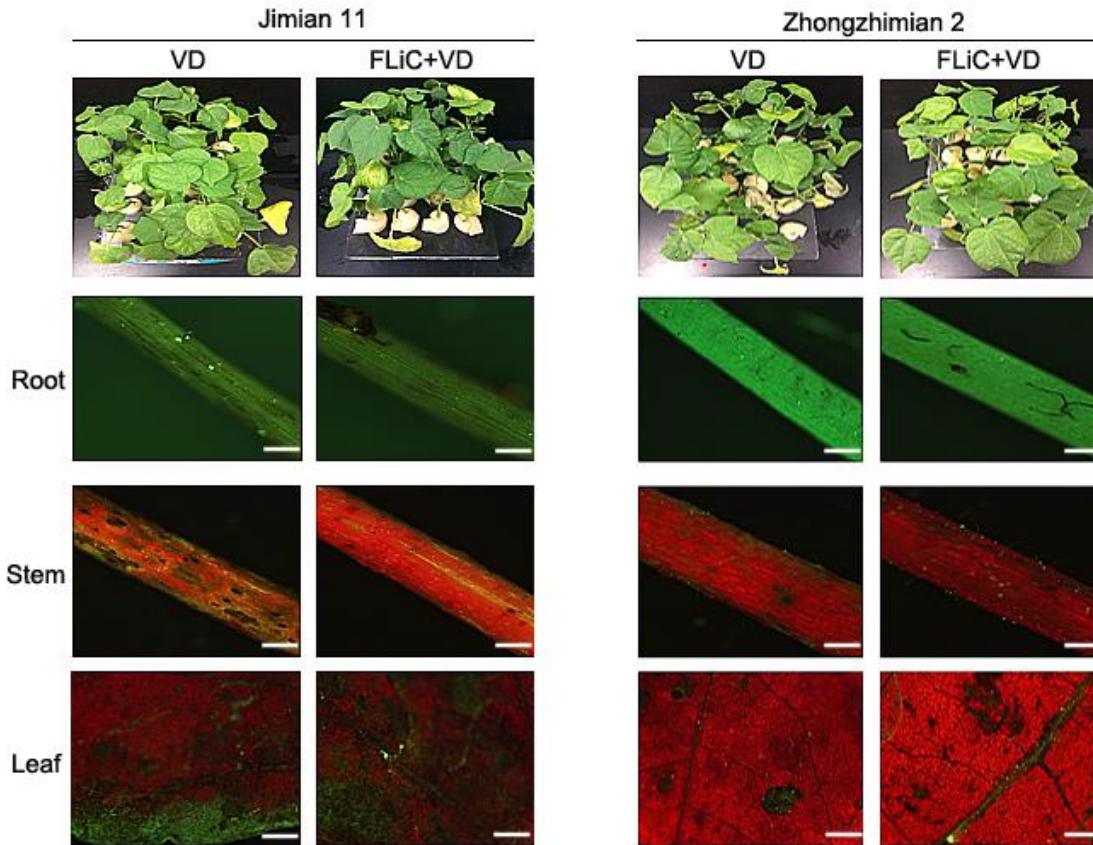


Figure 2 The effect of FLiC on the infection of VD in Jimian 11 and Zhongzhimian 2

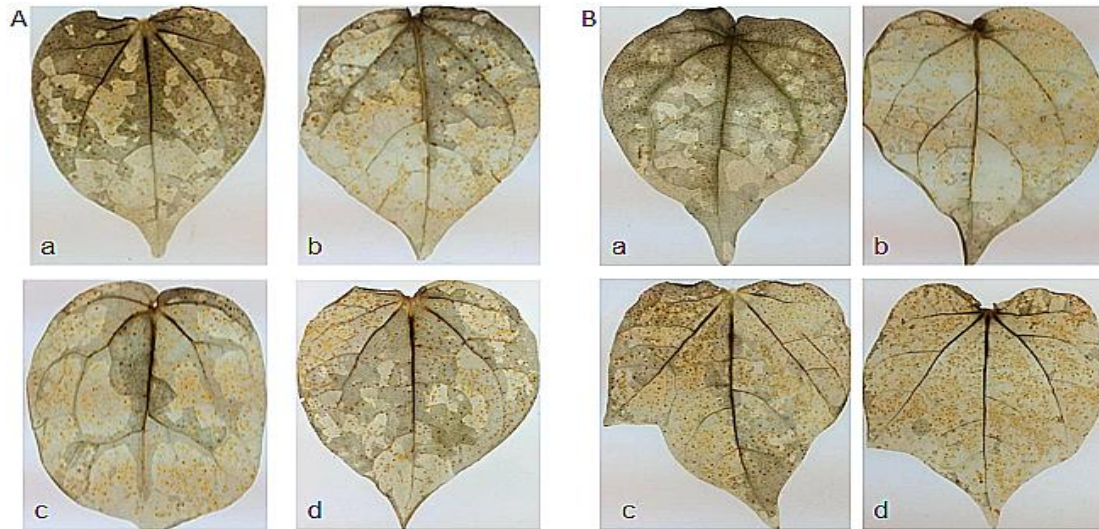
Table 1 FLiC induces disease resistance of different cotton varieties (30 d)

Treatment	Disease index(DI)	Relative control effect (%)
Jimian 11 (CK)	68.41±0.61a	
Jimian 11 (FLiC)	46.23±1.12c	32.42±1.39b
Zhongzhimian 2 (CK)	55.28±0.61b	
Zhongzhimian 2 (FLiC)	29.00±0.83d	47.50±2.09a

Note: Different letters indicate significant at the 0.05 level.

FLiC induces H₂O₂ accumulation in cotton

After FLiC and VD treated cotton leaves for 24 hours, a large amount of H₂O₂ could be clearly detected. Pretreatment of FLiC protein before VD treatment can induce more H₂O₂ deposition. However, the accumulation of H₂O₂ in Jimian 11 was less than that of Zhongzhimian 2. Therefore, FLiC can induce the outbreak of H₂O₂ in the leaves to induce the defense response of cotton, and the immune response of resistant varieties is stronger than that of susceptible varieties (Supplemental Figure S1).



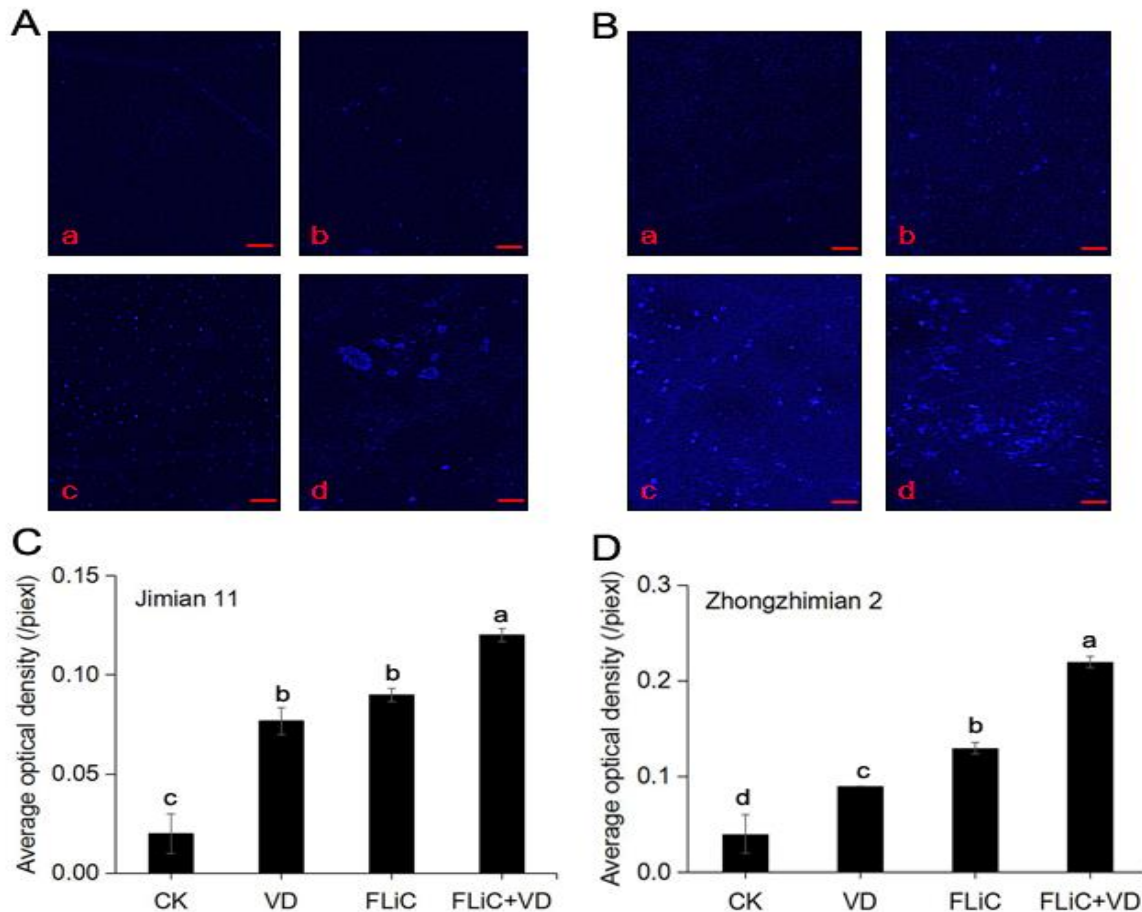
351
352 Supplemental Figure S1 FLiC induced the deposition of H₂O₂ in Jimian 11(A) and Zhongzhimian
353 2(B) leaves

354 a: Control; b: VD treatment; c: FLiC treatment; d: FLiC+VD treatment

355

356 **FLiC induces the accumulation of callose in cotton**

357 After FLiC treatment, both Jimian 11 and Zhongzhimian 2 can detect the obvious blue
358 fluorescent substance (Supplemental Figure S2). VD and FLiC treatments had little
359 difference in the corpus callosin content of Jimian 11, but significant difference in
360 Zhongzhimian 2. Pretreatment of FLiC before VD inoculation, resistant and susceptible
361 varieties produced a large amount of callus, and the induced resistance of resistant varieties
362 was higher than that of susceptible varieties. Therefore, FLiC can induce cotton leaves to
363 produce callose to enhance plant disease resistance.



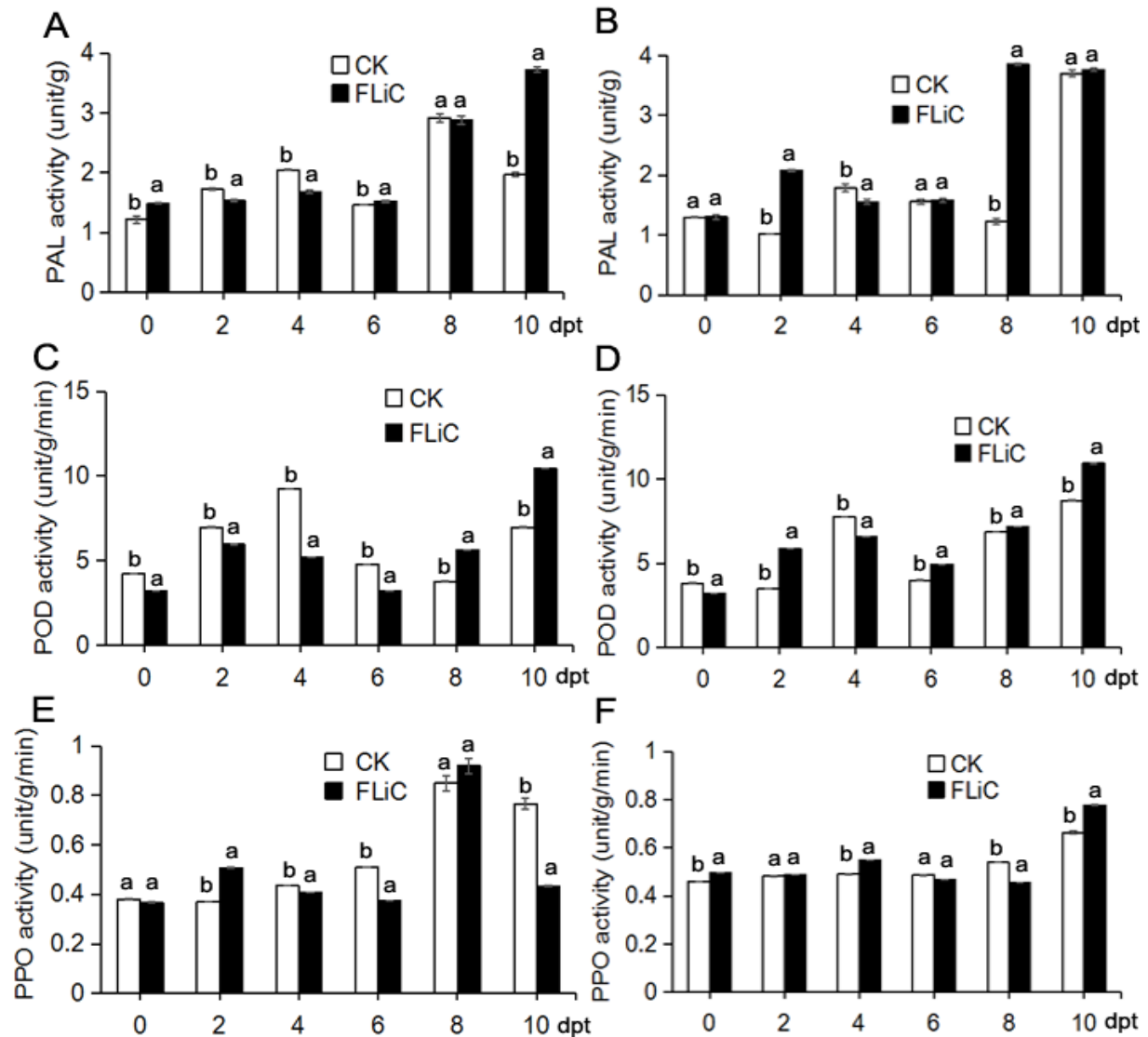
364
365 Supplemental Figure S2 FLiC-induced callose deposition in Jimian 11(A) and Zhongzhimian 2(B)
366 leaves; a: Control; b: VD treatment; c: FLiC treatment; d: FLiC+VD treatment; C: FLiC protein induces
367 the average optical density of Jimian 11 to accumulate callose; D: FLiC protein induces the average
368 optical density of Zhongzhimian 2 to accumulate callose; different letters indicate significant at the 0.05
369 level.

370

371 **FLiC-induced resistance depends on changes in related enzyme activities**

372 After FLiC treatment of Jimian 11 and Zhongzhimian 2 cotton seedlings, the activities
373 of the three defense-related enzymes in the cotton were increased to varying degrees. In
374 Jimian 11, the PAL activity reached the maximum at 10 d, while the resistant variety
375 reached the maximum at 8 d. The PAL activity in the resistant variety had a more obvious
376 response than the susceptible variety. The POD activity of susceptible varieties increased
377 significantly at 10 d, while the POD activity of resistant varieties peaked at 2 d, then

378 decreased to the control level after 6 d of inoculation, and peaked again after 10 d of
379 inoculation. The PAL activity of the susceptible varieties increased at 2 d, and there was no
380 significant difference from the control afterwards. The resistant varieties were higher than
381 the control at 4 d, and the PPO activity peaked at 10 d (Supplemental Figure S3). Therefore,
382 FLiC can induce different degrees of changes in the activities of three enzymes in cotton to
383 enhance disease resistance and more obvious disease-resistant varieties.



384 Supplemental Figure S3 FLiC induces the activity detection of defense-related enzymes in cotton
385 Jimian 11 (A, C, E) and Zhongzhimian 2 (B, D, F); different letters indicate significant at the 0.05 level.
386

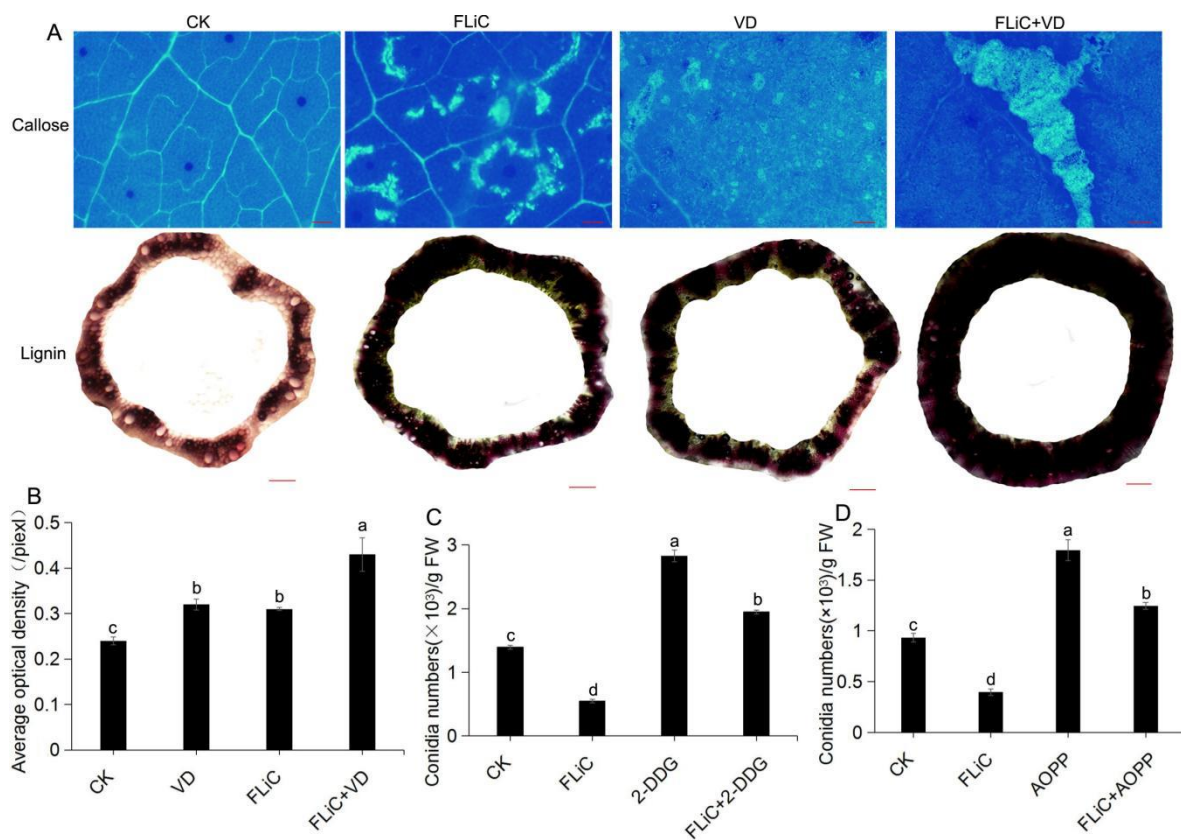
387

388 FLiC induces the deposition of callose and lignin

389 After applying FLiC to the leaves for 2 days, there were obvious callose deposits in

390 the leaves and the lignin content increased in the stems of Zhongzhimian 2 (Figure 3A).
391 This result is consistent with the result that FLiC induces callose deposits in resistant and
392 susceptible cotton. After pretreatment of FLiC before inoculation with VD, the deposition
393 of callus and lignin is more obvious. When 2-DDG and AOPP were pretreated, the amount
394 of callose and lignin deposition decreased, the amount of spores in the roots increased
395 significantly, and the FLiC induced resistance was weakened (Figure 3, C and D).
396 Therefore, FLiC can induce the deposition of lignin in stem cells and callose of leaves to
397 resist the infection of VD.

398



399 Figure 3 FLiC induces the deposition of lignin in cotton leaves and stems;(A) callose scale = 1000 μm ;
400 lignin scale = 2000 μm ; (B), The statistics of the average optical density of callose; (C), the statistics of
401 the bacterial mass after the corpus callose is cleared with 2-DDG; (D), the statistics of the bacterial mass
402 after the corpus lignin is cleared with AOPP; Different letters indicate significant at the 0.05 level.

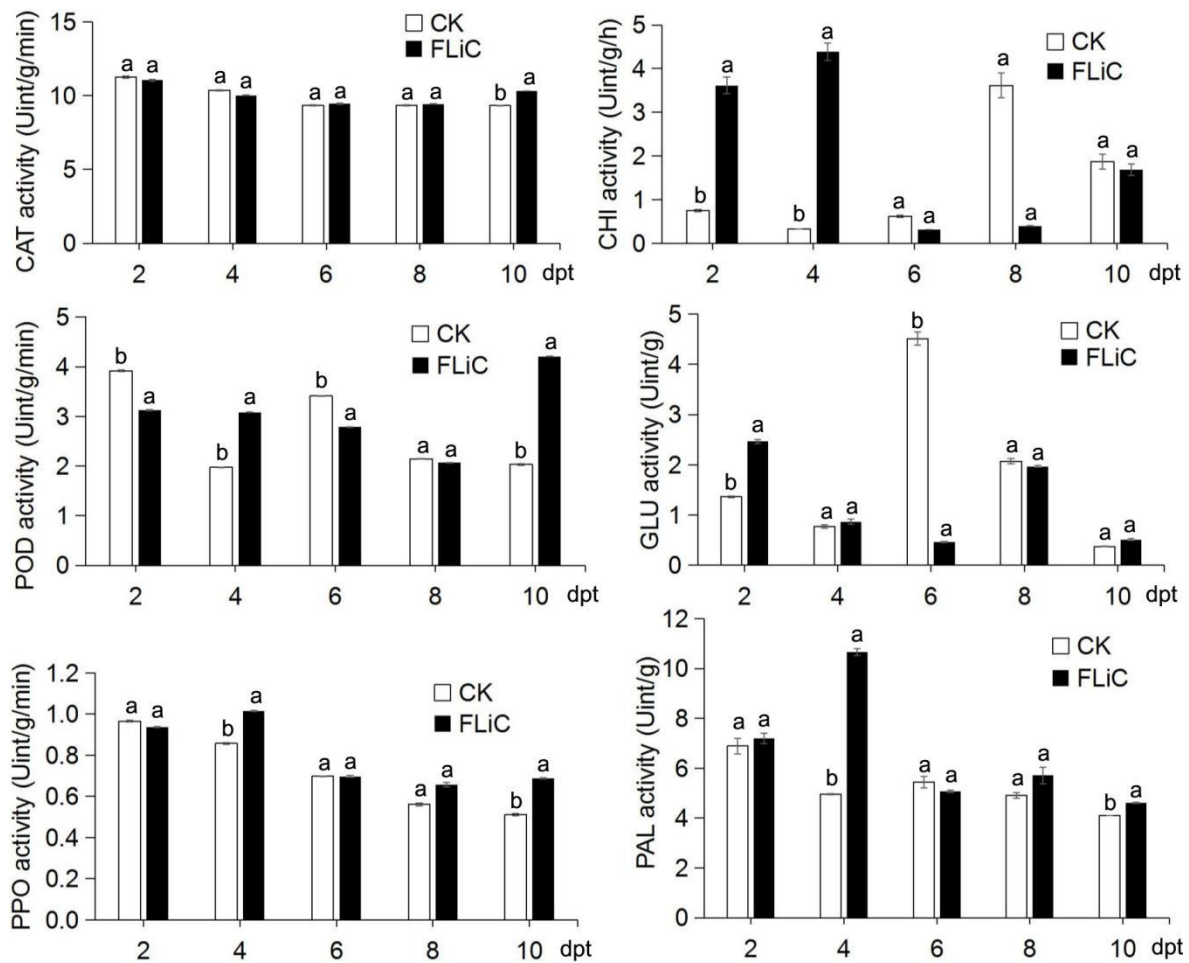
404

405

406 **FLiC-induced resistance depends on changes in defensive enzyme activity**

407 In order to further verify that FLiC can induce changes in enzyme activity in cotton to
408 enhance the defense response. We determined the changes in the activities of six enzymes
409 in the body of the disease-resistant variety Zhongzhimian 2 treated with FLiC alone. After
410 FLiC smeared the leaves, the activity of defense-related enzymes changed to varying
411 degrees (Supplemental Figure S4). CAT was significantly higher than the control on the
412 10th day. PPO, POD, and PAL all increased significantly on the 4th day compared with the
413 control, and on the 8th day after that they were comparable to the control, and on the 10th
414 day they all reached a significant level compared with the control. This result is basically
415 consistent with the changes in the activities of defense enzymes induced by FLiC in
416 resistant and susceptible cotton varieties. CHI reached a significant level compared with the
417 control on the 2nd and 4th day, and then began to drop to the control level. GLU increased
418 significantly on 2nd day compared with the control, and then began to decrease. This result
419 shows that after FLiC treatment, the activity of defense-related enzymes changes
420 differently under different induction time to improve disease resistance.

421



422

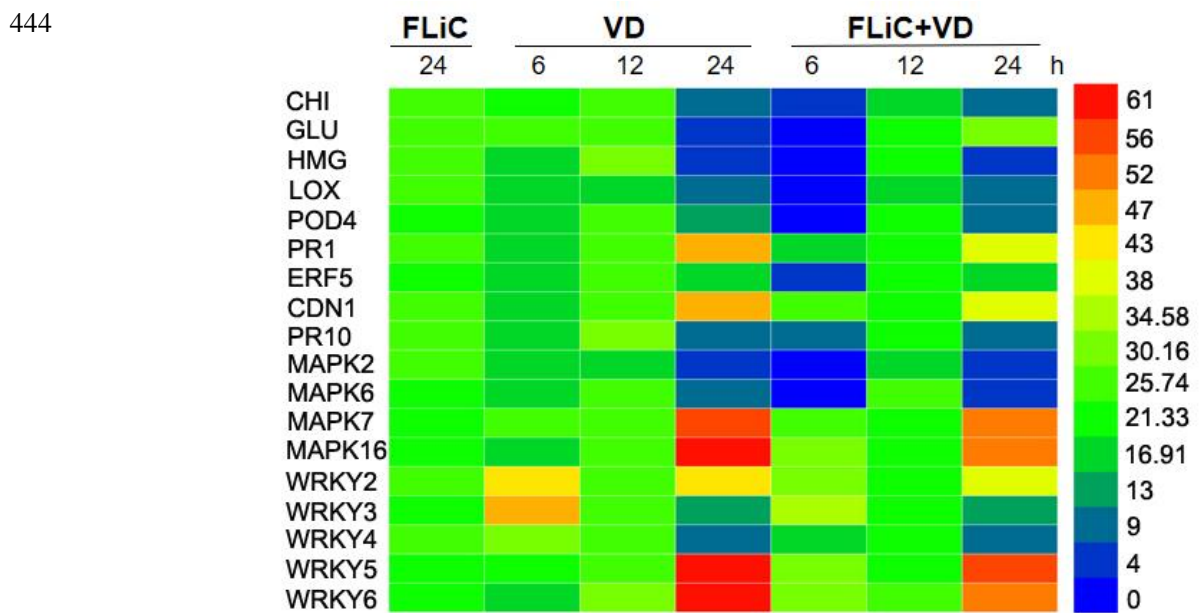
423

424 Supplemental Figure S4 FLiC induces changes in defense-related enzyme activities, the same letter
425 indicates that there is no significant difference at the 0.05 level.

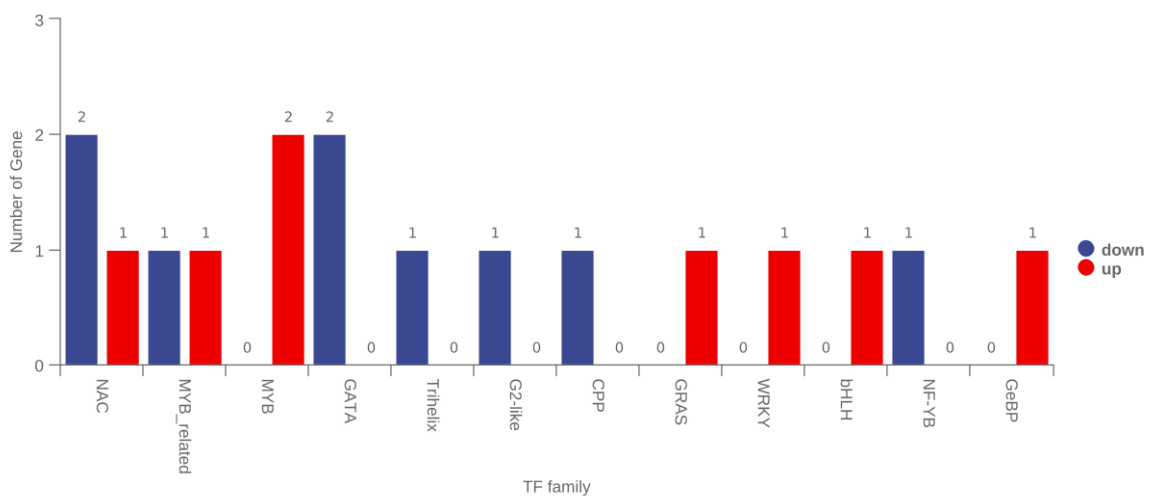
426 **FLiC induces the expression of disease resistance-related genes**

427 After the cotton seedlings were smeared with flagellin FLiC for 24 h, defense genes
428 such as *PR1*, *CHI*, *GLU*, *POD4*, *ERF5*, *PR10*, *LOX* and *CDN1* were induced to varying
429 degrees (Supplemental Figure S5). FLiC pretreated before inoculation with VD was the
430 treatment group, and only VD was inoculated as the control group. After 6 hours of
431 inoculation, the expression levels of *MAPK2*, *MAPK6* and *MAPK7* genes in the seedling
432 roots of the treatment group were lower than those of the control, and the expression levels
433 of the *MAPK16* gene were higher than those of the control. After 12 h and 24 h of
434 inoculation, the expression levels of *MAPK2*, *MAPK6*, *MAPK7* and *MAPK16* genes were
435 not significantly different from those of the control. It indicates that *MAPK16* gene may be

436 involved in the early immune response induced by FLiC. After 6 hours of inoculation with
 437 VD, the expression levels of *WRKY5* and *WRKY6* genes were higher than the control
 438 except for *WRKY2*, *WRKY3* and *WRKY4*. At 12 h and 24 h after inoculation, *WRKY2*,
 439 *WRKY3*, *WRKY4*, *WRKY5* and *WRKY6* were not significantly different from the control.
 440 These two transcription factors, *WRKY5* and *WRKY6*, may be involved in the early immune
 441 response induced by FLiC. This is consistent with the up-regulated expression of the
 442 differentially expressed transcription factor WRKY in the transcriptome results
 443 (Supplemental Figure S5).



445
 446 Supplemental Figure S5 Flagellin FLiC induced defence related genes expression
 447



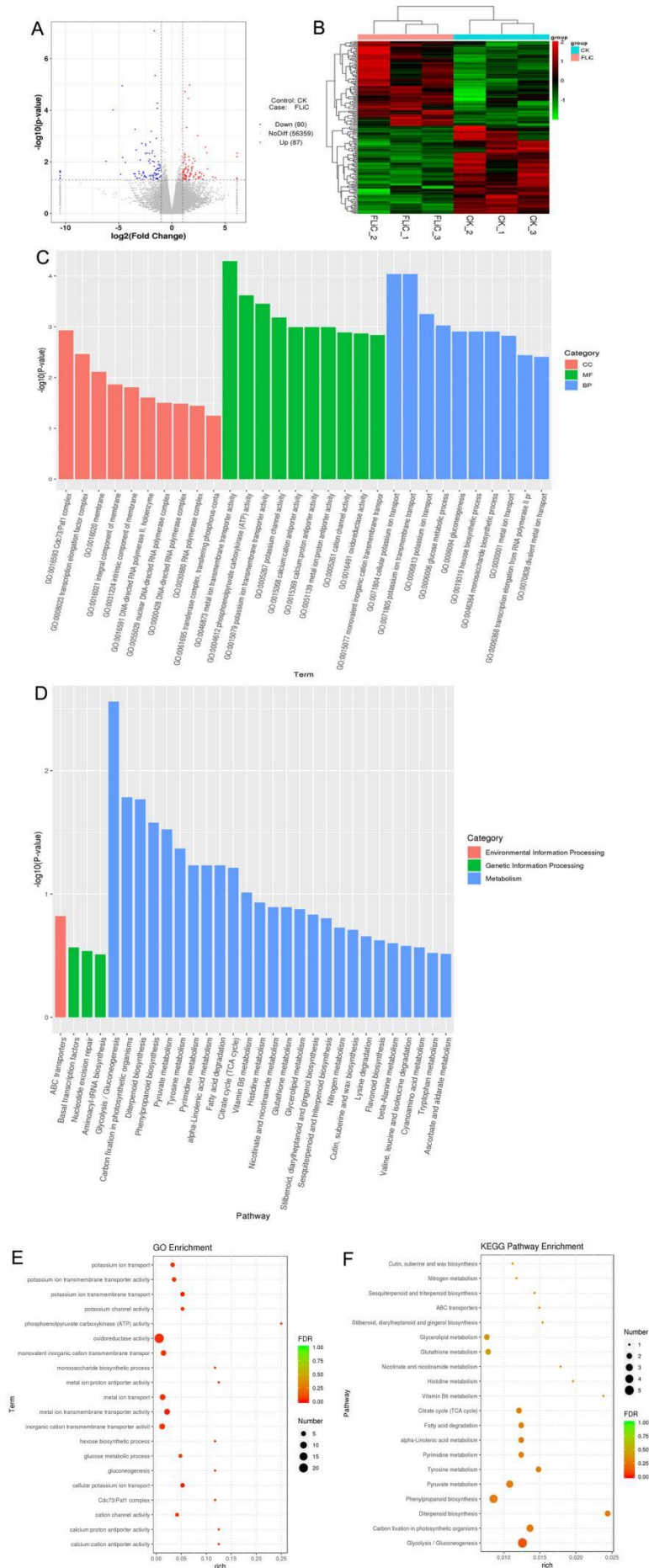
448

449 Supplemental Figure S6 Distribution of differentially expressed transcription factors in the
450 transcriptome

451 **Metabolic pathway enriched by differentially expressed genes in the**
452 **transcriptome**

453 The transcriptome results showed that 87 genes were up-regulated and 90 genes were
454 down-regulated. The significantly enriched differential genes were classified and clustered
455 as follows (Figure 4, A and B). Differentially expressed genes were significantly enriched
456 in related disease-resistant metabolic pathways such as potassium ion, calcium antiporter
457 activity, diterpenoid biosynthesis and phenylpropane biosynthesis (Figure 4, C-F).
458 Significantly enriched to two down-regulated calcium antiporter activity regulatory genes,
459 namely GH-A08G0063 and GH-D08G0067. Therefore, calcium antiporter activity
460 regulatory genes may negatively regulate plant disease resistance.

461

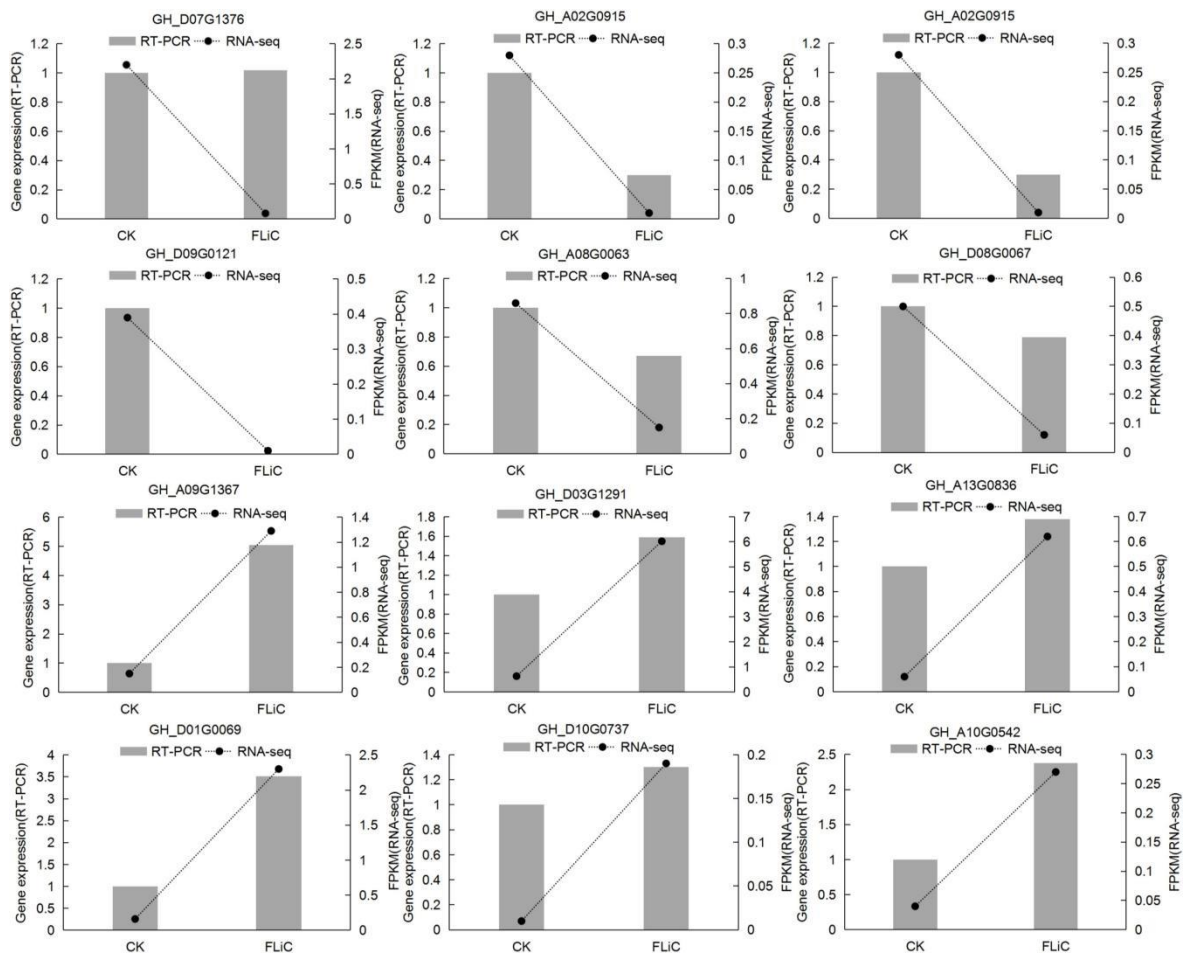


463 Figure 4 Pathways to which differentially expressed genes in the transcriptome are significantly
464 enriched; A, differential gene volcano map; B, differential gene cluster analysis; C, GO-enriched
465 metabolic pathway; D, KEGG-enriched metabolic pathway; E, The bubble chart of the first 20
466 metabolic pathways enriched by GO; F, the bubble chart of the first 20 metabolic pathways enriched by
467 KEGG. Note: C, the abscissa is the term of Go level 2, and the ordinate is the $-\log_{10}$ (p-value) enriched
468 for each term. D, the abscissa is the name of the pathway, and the ordinate is the $-\log_{10}$ (p-value)
469 enriched for each pathway.

470

471 RT-PCR verification of transcriptome results

472 Twelve groups were randomly selected from the RNA-seq sequencing results to verify
473 the transcriptome results by RT-PCR. The results showed that 11 of the 12 groups had the
474 same expression trend as the transcriptome, with an accuracy rate of 91.67%. It shows that
475 the transcriptome results are credible (Supplemental Figure S7).



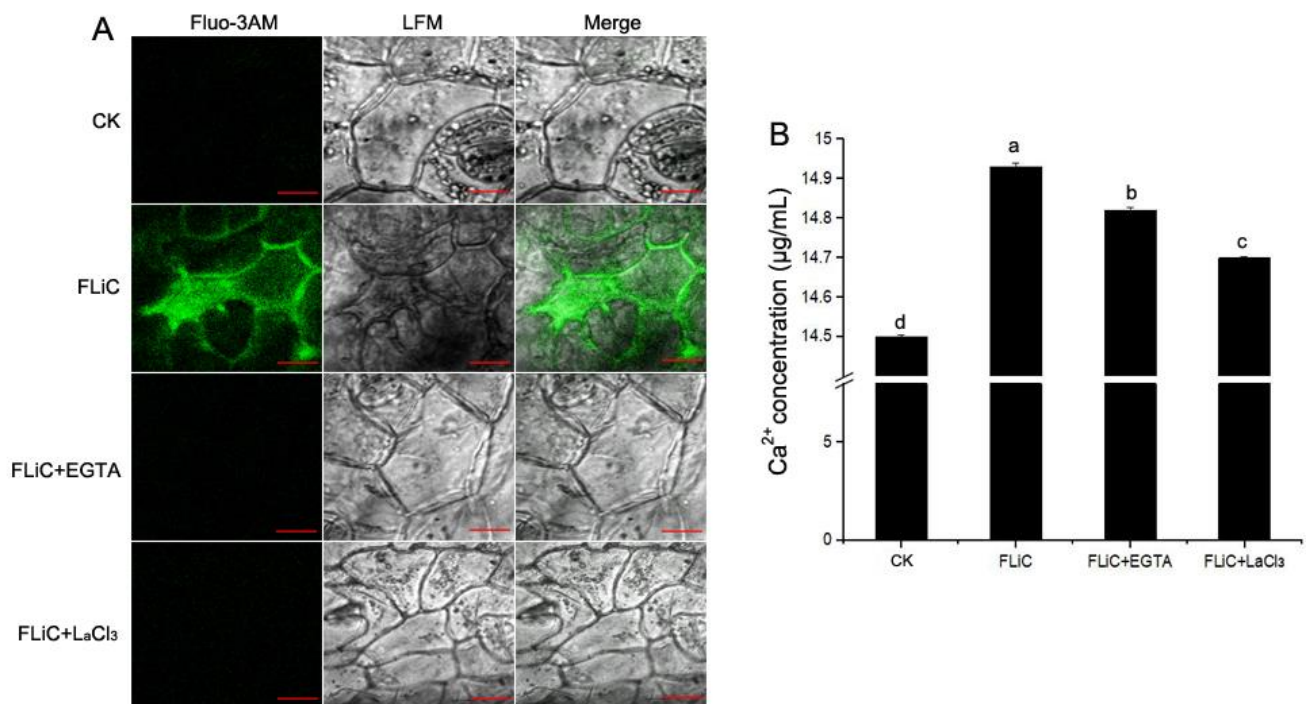
477 Supplemental Figure S7 Verification of FLiC transcriptome results

478

479 **The relationship between Ca²⁺, NO and H₂O₂**

480 **1. FLiC induces an increase in intracellular Ca²⁺**

481 According to the results of the transcriptome, the calcium antiporter activity was
482 significantly enriched. In order to verify that the FLiC protein induced resistance, the
483 increase in calcium ion influx caused the downstream immune response. The cotton
484 epidermal cells were loaded with Ca²⁺ sensitive fluorescent probe Fluo-3/aM, and then
485 FLiC protein at a concentration of 100 µg/mL was processed and observed with LSCM.
486 The results show that FLiC treatment can cause a significant increase in the fluorescence
487 intensity of epidermal cells (Figure 5). Pretreatment of Ca²⁺ chelating agent EGTA and Ca²⁺
488 channel blocker LaCl₃ significantly reduced the fluorescence intensity induced by FLiC.
489 Therefore, FLiC can induce the increase of Ca²⁺ concentration in cotton epidermal cells.
490 This is consistent with the results of calcium-related metabolic pathways that are
491 significantly enriched in the transcriptome.

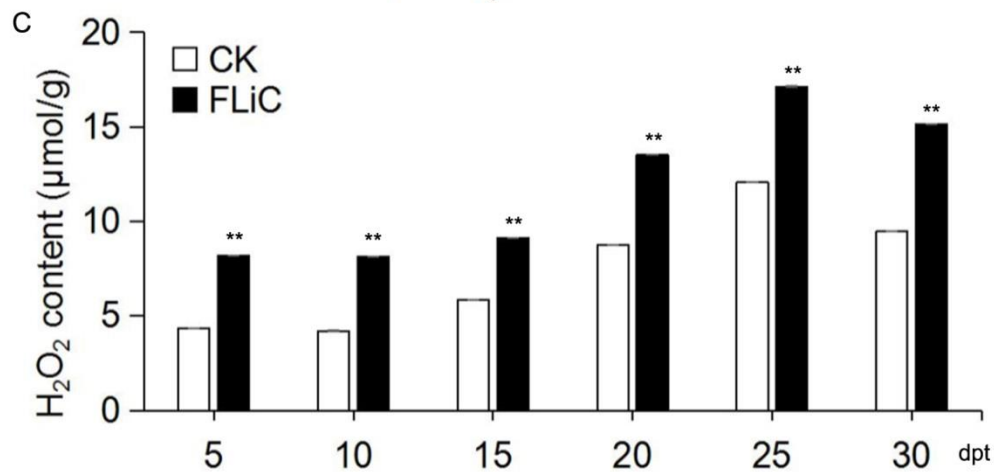
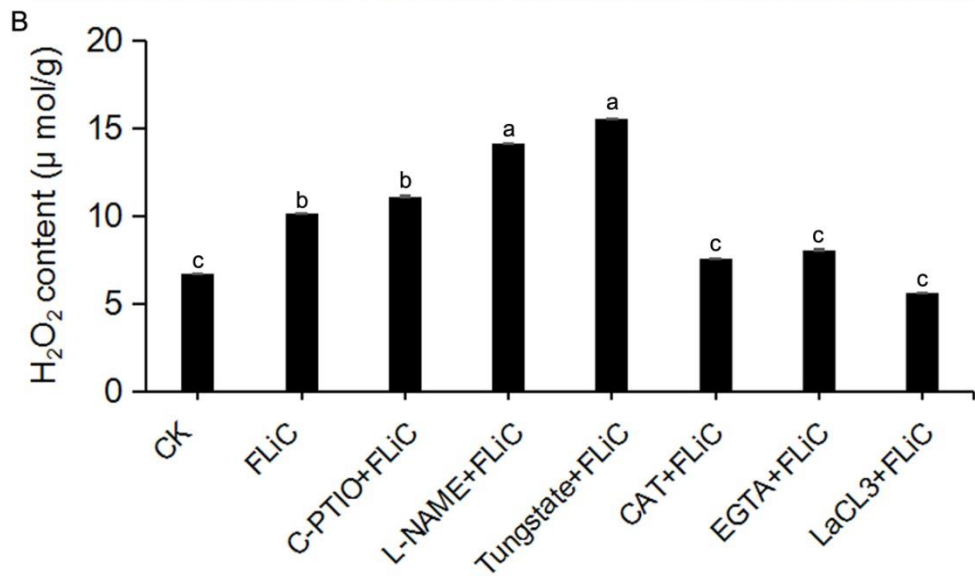
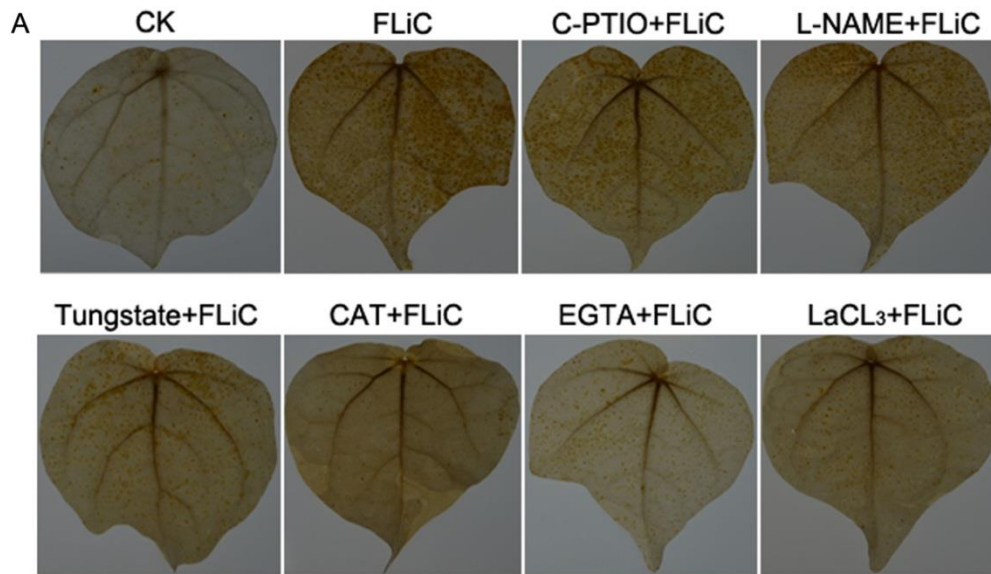


492

493 Figure 5 FLiC induces Ca^{2+} production in cotton epidermal cells; different letters indicate significant
494 differences at the 0.05 level; bar= 50 μm

495 **2. Different pretreatments affect the H_2O_2 burst induced by FLiC**

496 To determine the relationship between ROS, Ca^{2+} and NO. Two days after the FLiC
497 smearing treatment, there was an obvious burst of ROS in the leaves (Supplemental Figure
498 S8A). In order to study the influence of FLiC treatment on the relationship among Ca^{2+} ,
499 NO and H_2O_2 , after pretreatment of CAT, EGTA and LaCl_3 , the H_2O_2 content in the leaves
500 was significantly reduced to the control level. After pretreatment of C-PTIO, L-NAME and
501 Tungstate, the H_2O_2 content in the leaves was higher than that induced by FLiC alone
502 (Supplemental Figure S8B). The above results indicate that Ca^{2+} are located upstream of
503 H_2O_2 and affect the synthesis of H_2O_2 , while NO may be located beside or downstream of
504 H_2O_2 . After FLiC treatment for 5-30 days, the H_2O_2 in the leaves of the seedlings continued
505 to be significantly higher than that of the control. Until the 30th day, the H_2O_2 content
506 began to decrease, but it was still higher than the control (Supplemental Figure S8C).
507 Therefore, FLiC protein can induce cotton to produce an immune response and last longer.



508

509

510 Supplemental Figure S8 The effect of NO scavenger C-PTIO, NO synthesis inhibitor L-NAME and

511 sodium tungstate, H₂O₂ scavenger CAT, Ca²⁺ chelating agent EGTA and Ca²⁺ channel inhibitor LaCl₃ on

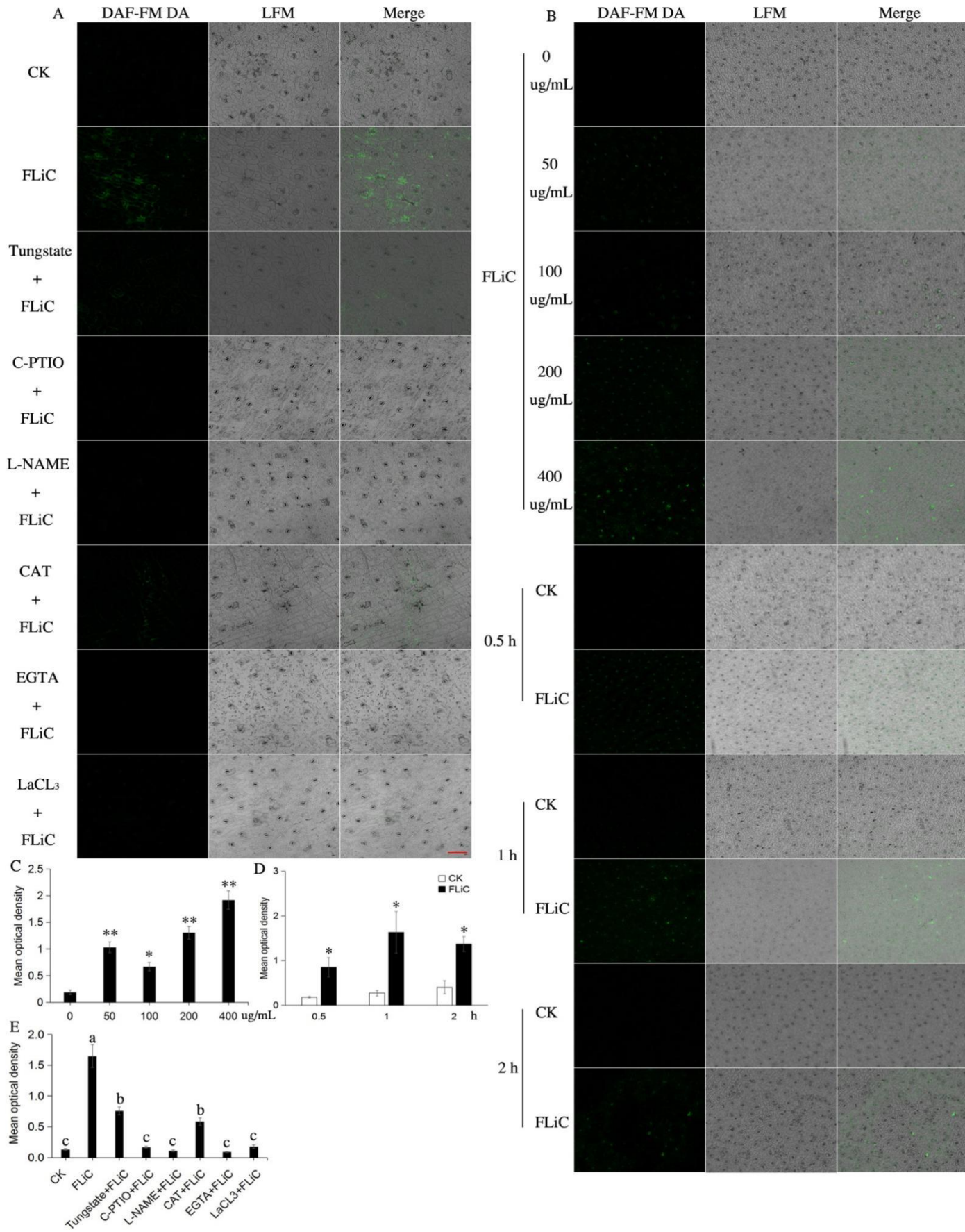
512 FLiC-induced H₂O₂ production. The brown substance represents the H₂O₂ in the leaves. Different letters

513 indicate significant differences at the 0.05 level.**, means that the difference is extremely significant at
514 the 0.01 level.

515

516 **3. FLiC induces NO production in cotton cells**

517 There was strong fluorescence around the epidermal cells and stomata of cotton
518 treated with FLiC, indicating that FLiC can induce the production of NO by cotton
519 epidermal cells (Figure 6A). When the concentration of FLiC was 400 $\mu\text{g}/\text{mL}$ and the
520 treatment for 1 h, the fluorescence intensity was the strongest (Figure 6B), indicating that
521 the production of NO induced by FLiC depends on the concentration of FLiC and the
522 treatment time. After pretreatment of NO scavenger C-PTIO and NOS pathway inhibitor
523 L-NAME, the fluorescence intensity decreased significantly (Figure 6A), indicating that
524 C-PTIO and L-NAME have an inhibitory effect on FLiC-induced NO production in
525 cotton epidermal cells. Nitrate reductase(NR) pathway inhibitor tungstate has only a
526 small inhibitory effect on FLiC-induced NO production in cotton epidermal cells. It
527 indicates that FLiC induces the production of NO by cotton epidermal cells, which may
528 be mainly synthesized through the nitric oxide synthase (NOS) pathway. After
529 pretreatment with CAT, EGTA and LaCl_3 , the NO content was significantly reduced. It
530 shows that Ca^{2+} and H_2O_2 are involved in the production of NO. Preliminary experiments
531 have shown that pretreatment of C-PTIO and L-NAME, FLiC can still induce more H_2O_2
532 production. It shows that NO has an inhibitory effect on FLiC-induced H_2O_2 . After
533 pretreatment of EGTA and LaCl_3 , the content of H_2O_2 is significantly reduced (Figure S8,
534 A and B). Therefore, in the immune response induced by FLiC, Ca^{2+} located upstream of
535 H_2O_2 and participate in the production of H_2O_2 . H_2O_2 will stimulate the production of
536 NO, and excessive NO will inhibit the production of H_2O_2 .



537

538

Figure 6 NO production in response to FLiC treatment in cotton leaves

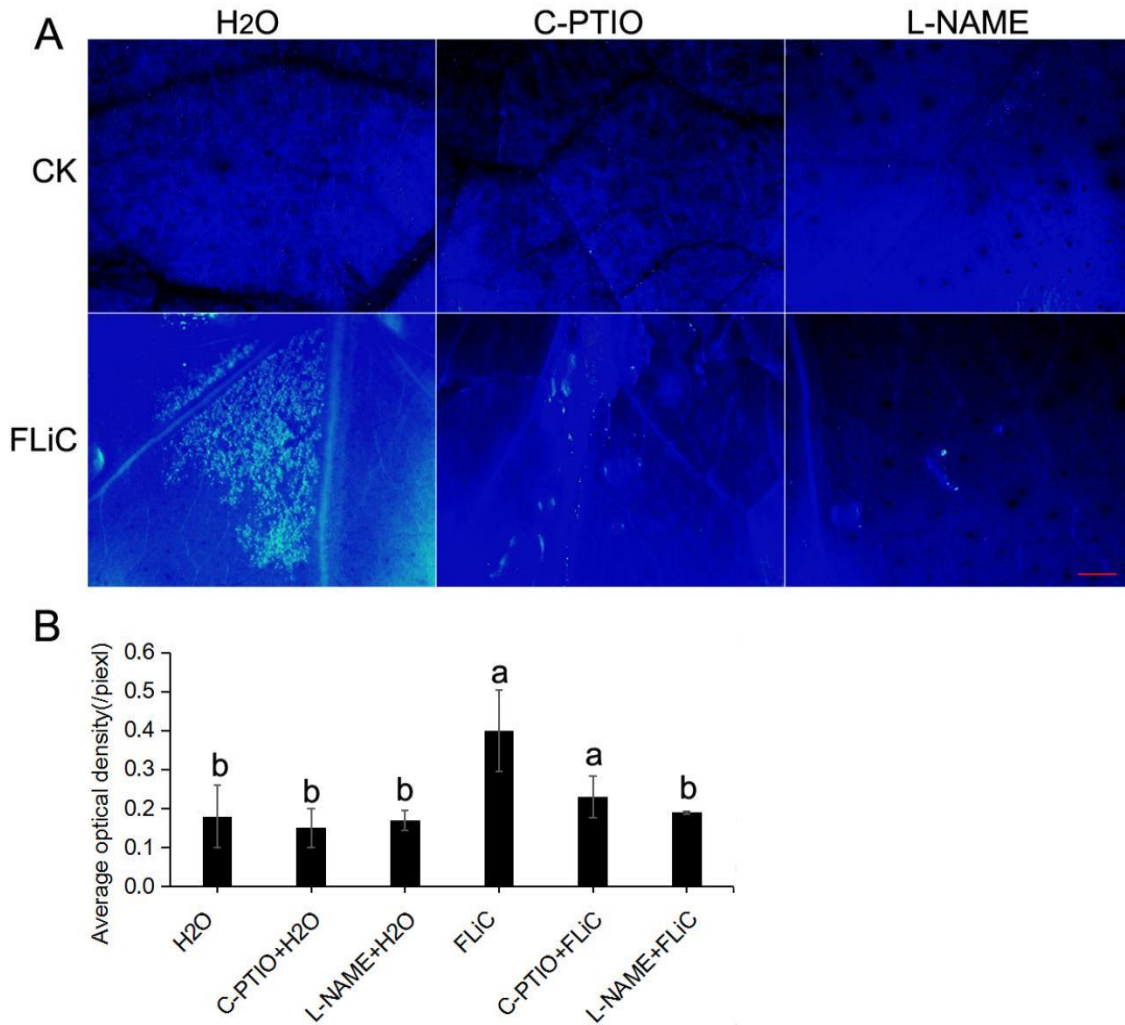
539 A. Fluorescence in cotton epidermal cells during different pretreatments (200 μ M C-PTIO, 200 μ M
540 L-NAME, 100 μ M tungstate, 100 unit/mL CAT, 5 mM EGTA and 200 μ M LaCl₃); B. Fluorescence
541 produced in cotton epidermal cells with different protein concentration and different treatment time; C.
542 The average fluorescence density of NO in cotton epidermal cells treated with different protein
543 concentrations; D. The average fluorescence density of NO in cotton epidermal cells after different
544 treatment time; E. The average fluorescence density of NO in cotton epidermal cells after different
545 pretreatments; *: The difference is significant at the 0.05 level; **: the difference is extremely significant
546 at the 0.01 level; different letters indicate that the difference between the treatments is significant at the
547 0.05 level; Bars = 20 μ m.

548

549 **NO is involved in FLiC-induced resistance**

550 **1. NO is involved in the deposition of callose induced by FLiC**

551 FLiC protein can induce callose in cotton leaves (Supplemental Figure S9), and after
552 pre-treatment of C-PTIO and L-NAME, FLiC-induced callose is significantly reduced
553 (Supplemental Figure S9). Therefore, the increase of callose induced by FLiC is dependent
554 on NO.



555

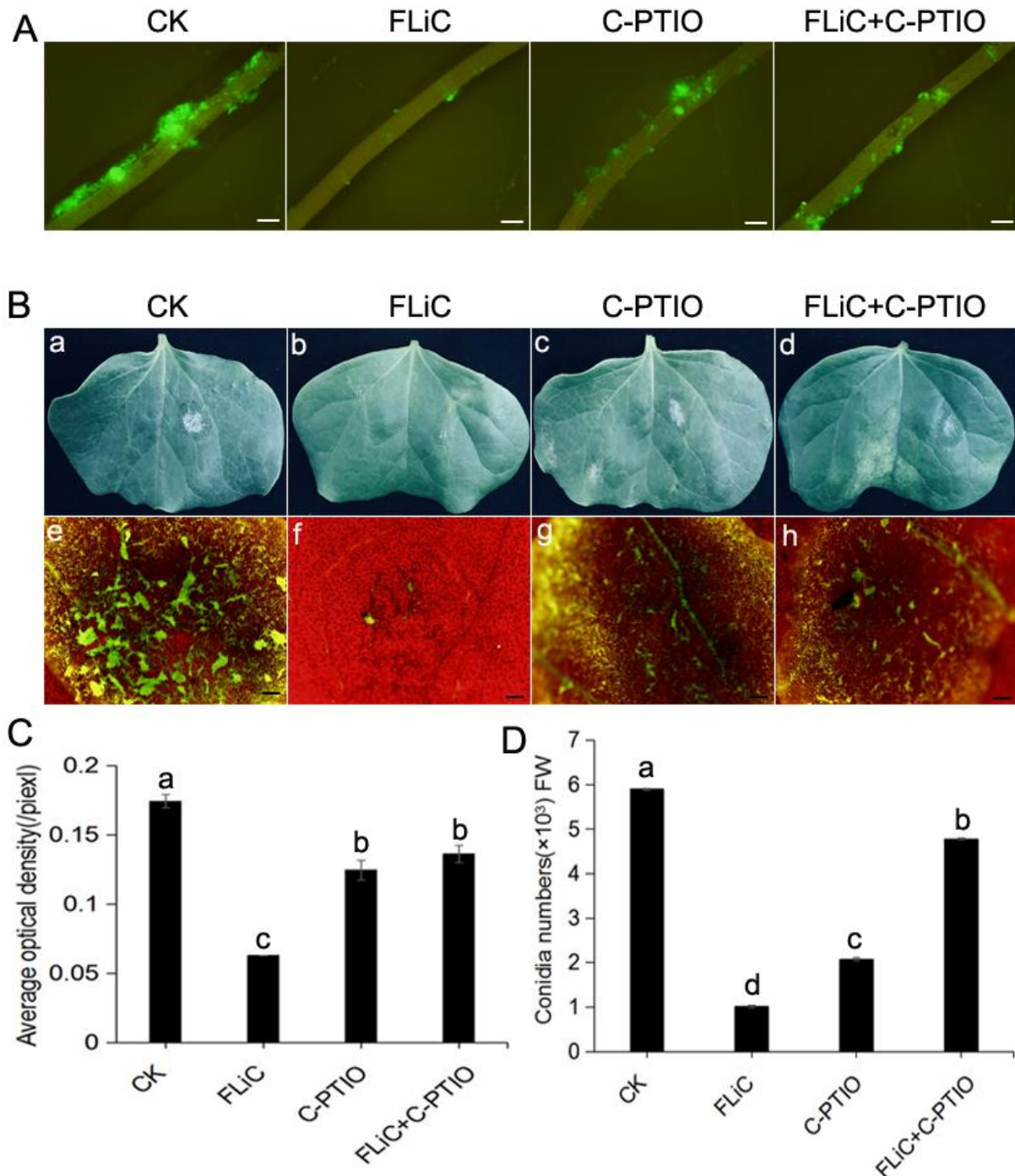
556

557 Supplemental Figure S9 NO is involved in the deposition of callose induced by FLiC; different letters
558 indicate significant at the 0.05 level; bars=500 μ m

559 2. NO reduces the damage of VD

560 After 48 hours of inoculation with VD, the number of pathogens colonizing the roots
561 of cotton seedlings pretreated with FLiC was significantly less than that of the control
562 (Supplemental Figure S10A). After pretreatment of C-PTIO, the number of pathogen
563 colonization increased, and the difference reached a significant level compared with the
564 control (Supplemental Figure S10D). Five days after the leaf was inoculated with spores of
565 VD, lesions were observed on the leaf surface (Supplemental Figure S10B). The disease
566 degree of the leaves of the seedlings treated with FLiC was significantly less than that of

567 the control. The area of leaf damage of pretreatment with C-PTIO, FLiC treatment and
568 control seedlings all increased. This result further indicates that the NO induced by FLiC
569 participates in the resistance of cotton to VD.



570
571 Supplemental Figure S10 NO is involved in FLiC-induced disease resistance
572 A. Colonization of fluorescently labeled VD on cotton roots. B. The infection of leaves inoculated
573 with VD under different treatments. a, b, c and d: leaf parts inoculated with VD. e, f, g and h:
574 observe the infection of VD on cotton cotyledons under a fluorescence microscope. C. The average

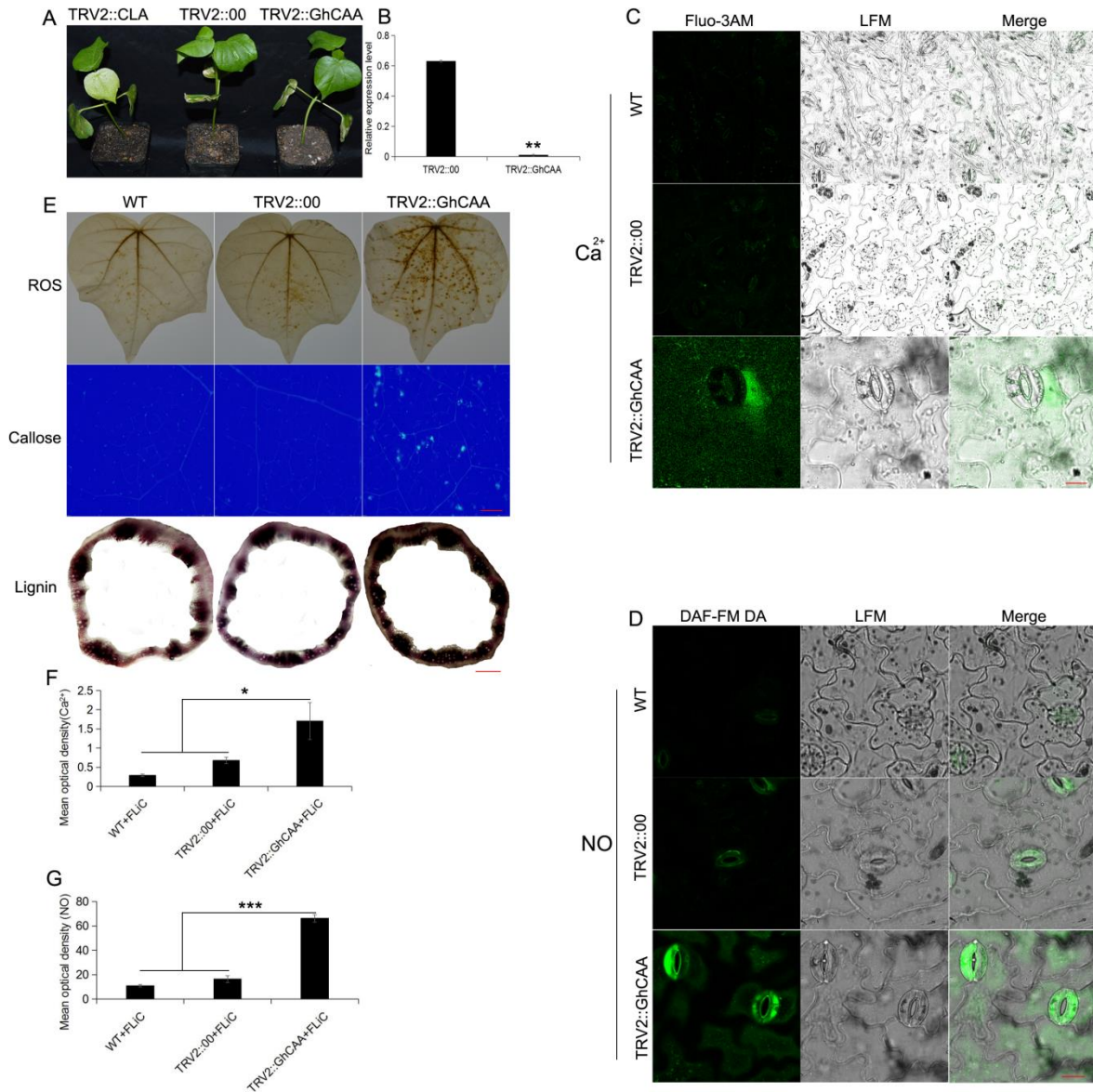
575 fluorescence density value of cotton roots. D. The number of spores on cotton roots. Different letters
576 indicate significant differences at the 0.05 level. Bars=500 μm .

577

578 **Calcium antiporter activity (GhCAA) increases in anti-disease**
579 **substances after silence**

580 In order to verify that the calcium antiporter activity regulatory gene negatively
581 regulates the disease resistance of cotton. After the positive control true leaves appeared
582 albino, the silencing efficiency of GhCAA was determined to reach 62% (Figure 7, A and
583 B). After the *GhCAA* gene was silenced, the intracellular Ca^{2+} and NO content in the
584 epidermis of cotton leaves after applying FLiC were significantly higher than that of WT
585 and TRV2::00 (Figure 7, C-G); The accumulation of ROS, callose and lignin was
586 significantly higher than that of WT and TRV2::00 (Figure 7E). Therefore, FLiC negatively
587 regulates the disease resistance of cotton by inhibiting the expression of *GhCAA* gene.

588



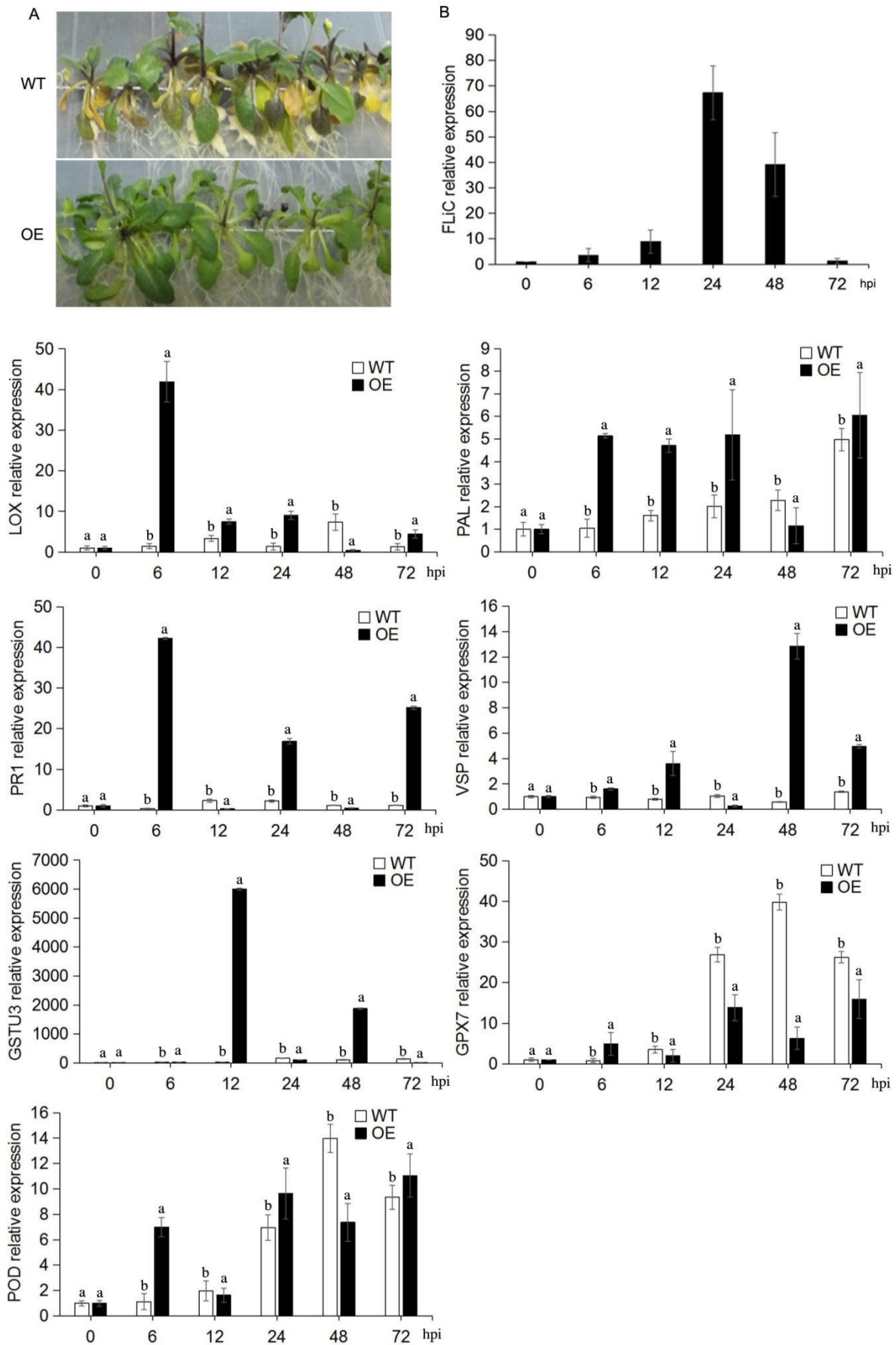
589
 590 Figure 7 Anti-disease substances increase after the silencing of the calcium antiporter activity gene
 591 *GhCAA*; *: The difference is significant at the 0.05 level; ***: the difference is extremely significant at
 592 the 0.001 level; C and D, bars= 50 μ m; E, bars= 2000 μ m.

593
 594 **Transgenic Arabidopsis with *FLiC* gene enhances resistance to VD and**
 595 **increases the expression of disease-resistant genes**

596 The *FLiC* gene-transformed Arabidopsis has enhanced disease resistance to VD
 597 (Supplemental Figure S11A). The expression of *FLiC* gene increased significantly at 24 h
 598 after inoculation (Supplemental Figure S11B). Therefore, transgenic *FLiC* gene

599 Arabidopsis can be highly expressed in vivo to improve plant disease resistance to VD. In
600 order to verify that *FLiC* gene-transformed Arabidopsis has enhanced resistance to VD, we
601 tested lipoxygenase (*LOX*), phenylalanine ammonia lyase (*PAL*), disease-related protein
602 (*PR1*) and vegetative storage protein (*VSP*). The expression of the four disease resistance
603 genes increased significantly. Therefore, *FLiC* gene-transformed Arabidopsis can
604 effectively increase the expression of disease resistance genes related to the SA and JA
605 signal pathways and enhance the plant's disease resistance. The expression level of
606 glutathione peroxidase gene (*GPX7*) showed no increasing trend or even lower than the
607 control; peroxidase (*POD*) was expressed more obviously when exposed to VD than the
608 control; glutathione sulfur transferase gene (*GSTU3*) expression increased significantly
609 (Supplemental Figure S11). Therefore, *FLiC* gene-transformed Arabidopsis can effectively
610 regulate the up-regulated expression of ROS and NO signal-related genes in plant roots and
611 enhance disease resistance.

612

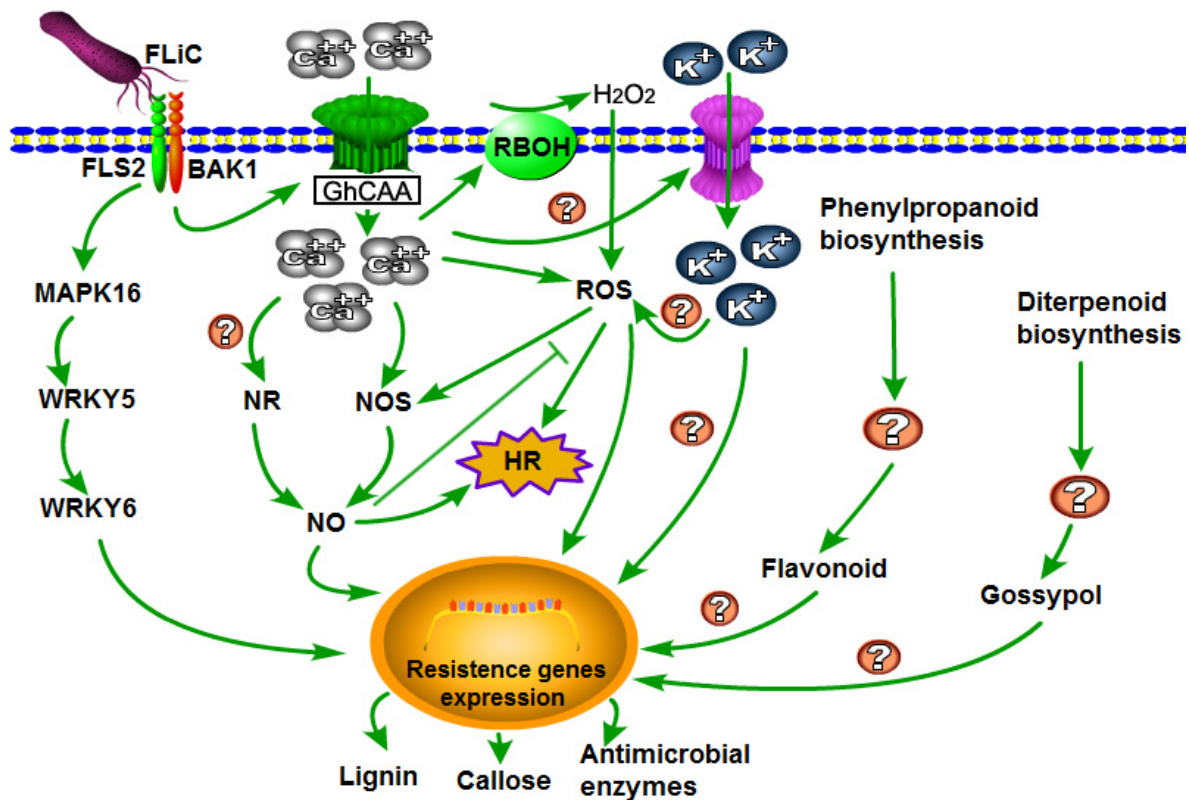


613

614

615 Supplemental Figure S11 A, *FLiC* gene-transformed *Arabidopsis* has enhanced disease resistance. B,
616 *FLiC* expression in transgenic *Arabidopsis thaliana* increased after inoculation; WT: wild type; OE: over
617 expression; *PAL*: phenylalanine ammonia lyase; *PRI*: disease-related protein; *LOX*: lipoxygenase; *VSP*:
618 vegetative storage protein; *GPX7*: glutathione peroxidase; *GSTU3*: glutathione sulfur transfer Enzyme
619 gene; *POD*: peroxidase; Different letters indicate significant differences at the 0.05 level.

620
621



622

623 Figure 8 Reasoning of FLiC-induced resistance signal pathway

624

625

626

627

628 **Discussion:**

629 **The metabolic pathways of FLiC protein and Flg22 protein to induce**
630 **immune response are different**

631 Rice is not sensitive to Flg22 but can recognize full-length flagellin (Takai, et al.,
632 2007). However, the mechanism by which full-length flagellin regulates the immune
633 response of plants is unclear. The effect and mechanism of FLiC full-length protein on
634 plant immune response have not been reported yet. Flg22 can induce immune response
635 effects in different plants, but there is no systematic metabolic pathway study in upland
636 cotton. We cloned a new type of flagellin gene *FLiC*, which contains the amino acid
637 sequence of Flg22. It can induce cotton to produce an immune response, such as the *MAPK*
638 cascade reaction and the up-regulation of key genes in disease resistance pathways such as
639 SA, JA, and ETH (Supplemental Figure S5). After the protein is treated with cotton, the
640 differentially expressed genes can be significantly enriched in potassium ions, calcium ions,
641 diterpenoid synthesis, phenylpropane biosynthesis, lignin biosynthesis, nitrogen
642 metabolism and other disease-resistant metabolic pathways through transcriptome analysis.
643 Therefore, the disease resistance induced by FLiC protein in cotton is related to the
644 activation of these pathways. We found that after silencing *GhCAA* on the membrane, the
645 intracellular Ca^{2+} content increased and induced NO, H_2O_2 and disease resistance related
646 substances to increase. It is clear that Ca^{2+} , NO and H_2O_2 are coordinately regulated to
647 enhance the resistance of cotton to VD (Figure 8). A 32 kDa flagellin Flg22 extracted from
648 *Pseudomonas syringae* can be used as an elicitor to induce defense responses in tomato
649 cells (Felix et al., 1999). Flg22 can induce a strong defense response in Arabidopsis,
650 including ROS bursts, callose deposition, ethylene production and the expression of
651 defense-related genes (Gómez-Gómez et al., 2000). Peroxidase-dependent oxidation burst
652 plays an important role in the basic resistance of *Arabidopsis thaliana* mediated by Flg22
653 recognition (Daudi et al., 2012; Liu et al., 2015). Nonexpresser of PR genes (*NPRI*) play a
654 role in the SA-induced initiation event, which enhances the oxidative burst triggered by
655 Flg22. This is related to the enhancement of callose deposition induced by Flg22 (Yi and

656 Kwon, 2014). Treatment of non-host plant tobacco with Flg22 will cause a strong defense
657 response, indicating that Flg22 is a PAMP that can act on a variety of plants and has a broad
658 spectrum of resistance (Nicaise, 2009). Therefore, our research not only found a new
659 full-length flagellin gene, but also used upland cotton as research material to explore a new
660 way to induce an immune response in plants and provide a new protein for cotton to resist
661 VD.

662

663 **Ca²⁺, NO and H₂O₂ synergistically enhance cotton disease resistance**

664

665 The relationship among Ca²⁺, NO and H₂O₂ in plants to regulate plant disease
666 resistance is still unclear. The interaction between the two to regulate the immune response
667 has been reported. NO not only participates in the regulation of plant growth and
668 development, but also participates in the signal transmission of plants in response to
669 various biotic and abiotic stresses (Yan et al., 2007; Sang et al., 2008; Martínez-Medina et
670 al., 2019). Ca²⁺ can activate the NO signal, and can also sense the NO signal. Ca²⁺
671 participates in the production of NO in tobacco and grapes induced by the elicitor, and the
672 NO produced can in turn cause the increase of intracellular Ca²⁺ concentration (Lamotte et
673 al., 2004; Vandelle et al., 2006; Besson-Bard et al., 2008). These indicate that there is an
674 interaction between Ca²⁺ and NO signals. it was found that an increase in
675 Ca²⁺ concentrations in mesophyll cells was necessary for the cells to produce ROS after
676 pathogen infection(Qiao et al., 2015). The synergistic effect of NO and H₂O₂ triggers the
677 death of hypersensitive cells. The absence of any one of this system cannot induce cell
678 death (Tada et al., 2004). Transient changes in the content of NO and H₂O₂ can activate a
679 series of physiological responses in plants, and they can interact to regulate the same or
680 related signal pathways to enhance a certain response. H₂O₂ can induce the synthesis and
681 accumulation of NO, and H₂O₂ regulates the NO content by affecting the activity of NO
682 synthase (Zhang et al., 2007). Similarly, NO can regulate H₂O₂ levels. H₂O₂ is involved in
683 mediating NO-induced resistance of tomato to *Rhizopus Nigricans*(Fan et al., 2008).
684 Ca²⁺ and H₂O₂ are involved in upstream of NO production to induce the HR cell death
685 (Qiao et al., 2015). However, it is not clear whether the content of NO negatively adjusts

686 the content of H₂O₂ . This study found that FLiC binds to membrane receptors and
687 negatively regulates calcium antiporter activity to increase the intracellular influx of Ca²⁺
688 and induce the production of H₂O₂ and NO; H₂O₂ acts as a signal molecule to induce the
689 production of NO, and NO inhibits the synthesis of H₂O₂; H₂O₂ and NO can induce the
690 production of defense responses. It shows that Ca²⁺、NO and H₂O₂ are synergistically
691 regulating the resistance of cotton to VD.

692

693 ***GhCAA* negatively regulates immune response**

694 No calcium antiporter-related regulatory genes have been found in cotton to negatively
695 regulate calcium ion levels and participate in cotton disease resistance. Bacterial flagellin is
696 the most in-depth study of PAMP (Wang, 2012). After Flg22 processes *Arabidopsis*
697 *thaliana*, the Ca²⁺ channel and its activation mechanism of stomatal closure in the process
698 of immune signal transduction indicate the specificity of the Ca²⁺ influx mechanism in
699 response to different stresses (Thor et al., 2020). HopZ-Activated Resistance 1 (ZAR1)
700 resistant body acts as a calcium permeable cation channel to trigger plant immunity and cell
701 death (Bi et al., 2021). After Flg22 treatment of *Arabidopsis thaliana*, the tonoplast
702 targeting pump *aca4/11* with double gene knockout showed higher basal Ca²⁺ levels and
703 higher amplitude Ca²⁺ signals than wild-type plants (Richard et al., 2020)。 It shows that
704 calcium transporter can negatively regulate calcium ion influx. The calcium transporter
705 *AtANN1* in *Arabidopsis thaliana* positively regulates the freezing tolerance of *Arabidopsis*
706 *thaliana* by affecting the influx of calcium signals mediated by low temperature (Liu et al.,
707 2021). Calcium transporter-related regulatory genes have positive regulation and negative
708 regulation of intracellular calcium ion levels to participate in plant defense
709 responses. Through transcriptome analysis, we found for the first time that calcium
710 antiporter activity related regulatory genes negatively regulate calcium levels to enhance
711 cotton resistance to VD.

712

713 ***FLiC*-transformed *Arabidopsis* has enhanced resistance to VD**

714 In order to verify whether the *FLiC* gene-transformed *Arabidopsis* can improve the
715 resistance to VD. Transformation of flagellin gene can improve rice resistance to bacterial
716 streaks(Wang et al., 2014). The flagellin gene of *Bacillus subtilis* was transferred into rice
717 to increase the resistance to rice blast and the genetically modified rice leaves produced
718 allergic reaction spots (Wang et al., 2015). After the *FLiC* gene *Arabidopsis* was inoculated
719 with VD, the relative expression levels of SA and JA defense signal-related genes *LOX*,
720 *PAL*, *PRI*, and *VSP* all increased significantly, and the expression levels of *LOX* and *PRI*
721 both reached 40 times. The expression of genes *GSTU3*, *GPX7* and *POD* related to ROS
722 and NO signal pathway changed to varying degrees. Therefore, transgenic *Arabidopsis* with
723 *FLiC* gene can induce the expression of key genes in SA, JA, ROS and NO signaling
724 pathways to improve plant disease resistance.

725
726 **Acknowledgments:** This work was financially supported by the National Key R & D
727 Program of China (2016YFD0102105) and the Postgraduate Research & Practice
728 Innovation Program of Jiangsu Province (KYCX20_0582).

729
730 **Conflict of interest:** The authors declare that they have no conflict of interest.

731
732 **Author Contributions** Heng Zhou: responsible for the concepts, design, definitions of
733 intellectual content, literature search, data analysis and manuscript preparation. Yijing Xie:
734 provided assistance for data acquisition and data analysis. Yi Wang: carried out the
735 literature search and data acquisition. Heqin Zhu and Canming Tang: performed manuscript
736 editing and manuscript review. All authors have read and approved the content of the
737 manuscript.

738

739

740

741

742

743

744

745

746

747 References

748 **Abeles FB, Forrence LE** (1970) Temporal and hormonal control of beta-1, 3-glucanase in *Phaseolus*
749 *vulgaris* L. *Plant Physiol* **45**: 395–400

750
751 **Ali MB, Singh N, Shohael AM, et al.** (2006) Phenolics metabolism and lignin synthesis in root
752 suspension cultures of *Panax ginseng* in response to copper stress[J]. *Plant Science* **171**: 147-154.

753
754 **Asai T, Tena G, Plotnikova J, et al.** (2002) MAP kinase signaling cascade in *Arabidopsis* innate
755 immunity. *Nature* **415**: 977-983

756
757 **Besson-Bard A, Courtois C, Gauthier A, Dahan J, Dobrowolska G, Jeandroz S, Pugin A,**
758 **Wendehenne D** (2008) Nitric oxide in plants: production and cross-talk with Ca^{2+} signaling. *Mol Plant*
759 **1**:218-228

760
761 **Bi G, Su M, Li N, Liang Y, Dang S, Xu J, Hu M, Wang J, Zou M, Deng Y, Li Q, Huang S, Li J,**
762 **Chai J, He K, Chen YH, Zhou JM** (2021) The ZAR1 resistosome is a calcium-permeable channel
763 triggering plant immune signaling. *Cell* **184**:3528-3541

764
765 **Bouizgarne B, El-Maarouf-Bouteau H, Frankart C, et al.** (2006) Early physiological responses of
766 *Arabidopsis thaliana* cells to fusaric acid: toxic and signalling effects. *The New Phytologist* **169**:
767 209-218

768
769 **Brennan T, Frenkel C** (1977) Involvement of hydrogen peroxide in the regulation of senescence in pear.
770 *Plant Physiol* **59**: 411–416

771
772 **Bright J, Desikan R, Hanecek J T, Weir1 S, Neill S J** (2006) ABA induced NO generation and
773 stomatal closure in *Arabidopsis* are dependent on H_2O_2 synthesis. *The Plant J* **45**:113-122

774
775 **Buxdorf K, Rahat I, Gafni A, Levy M** (2013) The epiphytic fungus *Pseudozyma aphidis* induces
776 jasmonic acid- and salicylic acid/nonexpressor of PR1-independent local and systemic resistance. *Plant*
777 *Physiol* **161**:2014-2022

778
779 **Chen YL, Huang R, Xiao YM, Lü P, Chen J, Wang XC** (2004) Extracellular calmodulin-induced
780 stomatal closure is mediated by heterotrimeric G protein and H_2O_2 . *Plant Physiol* **136**: 4096–4103

781
782 **Daudi A, Cheng Z, O'Brien JA, Mammarella N, Khan S, Ausubel FM, Bolwell GP** (2012) The
783 apoplastic oxidative burst peroxidase in Arabidopsis is a major component of pattern-triggered immunity.
784 *Plant Cell* **24**:275-87
785
786 **Dickerson DP, Pascholati SF, Hagerman AE, Butler LG, Nicholson RL** (1984) Phenylalanine
787 ammonia-lyase and hydroxy cinnamate: CoA ligase in maize mesocotyls inoculated with
788 *Helminthosporium maydis* or *Helminthosporium carbonum*. *Physiol Plant Pathol* **25**: 111–123
789
790 **Dixon RA, Harrison MJ, and Lamb CJ** (1994) Early events in the activation of plant defense
791 responses. *Annual Review of Phytopathology* **32**: 479-501
792
793 **Dong H, Li W, Zhang D, et al.** (2003) Differential expression of induced resistance by an aqueous
794 extract of killed *Penicillium chrysogenum* against *Verticillium* wilt of cotton[J]. *Crop Protection* **22**:
795 129-134.
796
797 **Durrant WE, Dong X**(2004) Systemic acquired resistance. *Annual Review of Phytopathology* **42**:
798 185-209
799
800 **Ebel J, Mithöfer A** (1998) Early events in the elicitation of plant defence. *Planta* **206**: 335-348
801
802 **Emani C, Garcia JM, Lopata-Finch E, Pozo MJ, Uribe P, KimDJ, Sunilkumar G, Cook DR,**
803 **Kenerley CM, Rathore KS** (2003) Enhanced fungal resistance in transgenic cotton expressing an
804 endochitinase gene from *Trichoderma virens*. *Plant Biotechnol J* **1**: 321–336
805
806 **Fan B, Shen L, Liu KL, et al.** (2008) Interaction between nitric oxide and hydrogen peroxide in
807 postharvest tomato resistance response to *Rhizopus Nigricans*. *J Sci Food Agric* **88**: 1238-1244
808
809 **Felix G, DuranJ D, Volko S, et al.** (1999) Plants have a sensitive perception system for the most
810 conserved domain of bacterial flagellin. *Plant Journal* **18**: 265-276
811
812 **Gómez-Gómez L, Boller T** (2000) FLS2: an LRR receptor-like kinase involved in the perception of the
813 bacterial elicitor flagellin in Arabidopsis. *Molecular Cell* **5**: 1003-1011
814

- 815 **Han Q** (2014) Screening and identification of cotton anti-VD biocontrol bacteria and research on
816 disease resistance mechanism. Nanjing: Nanjing Agricultural University
817
- 818 **Holmes EC, Chen YC, Mudgett MB, Sattely ES.** (2021) Arabidopsis UGT76B1 glycosylates
819 N-hydroxy-pipecolic acid and inactivates systemic acquired resistance in tomato. *Plant Cell* **33**:750-765
820
- 821 **Hu HL** (2012) Construction of transgenic VD with GFP gene and study on the process of infecting
822 cotton. Nanjing Agricultural University
823
- 824 **Jennings JC, Birkhold PC, Mock NM** (2001) Induction of defense responses in tobacco by the protein
825 Nep1 from *Fusarium oxysporum*. *The Plant Science* **161**: 891-899
826
- 827 **Jones JD, Dangl JL** (2006) The plant immune system. *Nature* **444**: 323-329
828
- 829 **Kumar R, Barua P, Chakraborty N, Nandi AK** (2020) Systemic acquired resistance specific proteome
830 of *Arabidopsis thaliana*. *Plant Cell Rep* **39**:1549-1563
831
- 832 **Kumar V, Parkhi V, Kenerley CM, et al.** (2009) Defense-related gene expression and enzyme
833 activities in transgenic cotton plants expressing an endochitinase gene from *Trichoderma virens* in
834 response to interaction with *Rhizoctonia solani*. *Planta* **230**: 277-291
835
- 836 **Lamotte O, Gould K, Lecourieux D, Sequeira-Legrand A, Lebrun -Garcia A, Durner J,**
837 **Pugin A & Wende-henne D** (2004) Analysis of nitric oxide signaling functions in tobacco cells
838 challenged by the elicitor cryptogein . *Plant Physiol* **135**: 516-529
839
- 840 **Li B, Fu Y, Jiang D, Xie J, Cheng J, Li G, Hamid MI, Yi X** (2010) Cyclic GMP as a second
841 messenger in the nitric oxide-mediated conidiation of the mycoparasite *Coniothyrium minitans*. *Appl*
842 *Environ Microbiol* **76**: 2830–2836
843
- 844 **Liu P, Zhang H, Yu B, Xiong L, Xia Y** (2015) Proteomic identification of early salicylate- and
845 flg22-responsive redox-sensitive proteins in *Arabidopsis*. *Sci Rep* **27**:8625
846
- 847 **Liu Q, Ding Y, Shi Y, Ma L, Wang Y, Song C, Wilkins KA, Davies JM, Knight H, Knight MR,**
848 **Gong Z, Guo Y, Yang S** (2021) The calcium transporter ANNEXIN1 mediates cold-induced calcium

- 849 signaling and freezing tolerance in plants. *EMBO J* **40**:e104559
850
- 851 **Livak KJ, Schmittgen TD** (2001) Analysis of relative gene expression data using real-time quantitative
852 PCR and the $2^{-\Delta\Delta CT}$ Method. *Methods* **25**: 402–408
853
- 854 **Martínez-Medina A, Pescador L, Terrón-Camero LC, Pozo MJ, Romero-Puertas MC** (2019) Nitric
855 oxide in plant-fungal interactions. *J Exp Bot* **70**:4489-4503
856
- 857 **Millet Y A, Danna C H, Clay N K, et al.** (2010) Innate immune responses activated in Arabidopsis
858 roots by microbe-associated molecular patterns. *Plant Cell* **22**: 973-990
859
- 860 **Naveed ZA, Wei X, Chen J, Mubeen H, Ali GS** (2020) The PTI to ETI Continuum
861 in Phytophthora-Plant Interactions. *Front Plant Sci* **17**: 593965
862
- 863 **Nicaise V, Roux M, Zipfel C** (2009) Recent advances in PAMP-triggered immunity against bacteria:
864 pattern recognition receptors watch over and raise the alarm. *Plant Physiol* **150**: 1638-1647
865
- 866 **Nürnberg T, Brunner F** (2002) Innate immunity in plants and animals: emerging parallels between
867 the recognition of general elicitors and pathogen-associated molecular patterns. *Current Opinion in Plant*
868 *Biology* **5**: 318-324
869
- 870 **Plazek A, Zur I** (2003) Cold-induced plant resistance to necrotrophic pathogens and antioxidant enzyme
871 activities and cell membrane permeability. *Plant Sci* **164**: 1019–1028
872
- 873 **Pomar F, Merino F, Barceló A R** (2002) O-4-Linked coniferyl and sinapyl aldehydes in lignifying cell
874 walls are the main targets of the Wiesner (phloroglucinol-HCl) reaction. *Protoplasma* **220**: 17-28
875
- 876 **Qiao M, Sun J, Liu N, Sun T, Liu G, Han S, Hou C, Wang D** (2015) Changes of Nitric Oxide and Its
877 Relationship with H₂O₂ and Ca²⁺ in Defense Interactions between Wheat and Puccinia Triticina. *PLoS*
878 *One* **10**:e0132265
879
- 880 **Ren A, Li MJ, Shi L, Mu DS, Jiang AL, Han Q, Zhao MW** (2013) Profiling and quantifying
881 differential gene transcription provide insights into ganoderic acid biosynthesis in *Ganoderma lucidum*
882 in response to methyl jasmonate. *PLoS One* **8**: e65027

- 883
- 884 **Richard Hilleary, Julio Paez-Valencia, Cullen Vens, Masatsugu Toyota, Simon Gilroy** (2020)
- 885 Tonoplast-localized Ca²⁺ pumps regulate Ca²⁺ signals during pattern-triggered immunity in *Arabidopsis*
- 886 *thaliana*. Proceedings of the National Academy of Sciences **117**:18849-18857
- 887
- 888 **Sang J, Jiang M, Lin F, et al.** (2008) Nitric oxide reduces hydrogen peroxide accumulation involved in
- 889 water stress-induced subcellular antioxidant defense in maize plants. J Integr Plant Biol **50**: 231-243
- 890
- 891 **Sudhakar C, Lakshmi A, Giridarakumar S** (2001) Changes in the antioxidant enzyme efficacy in two
- 892 high yielding. Plant Sci **161**: 613– 619
- 893
- 894 **Sun A, Nie S, Xing D** (2012) Nitric oxide-mediated maintenance of redox homeostasis contributes to
- 895 NPR1-dependent plant innate immunity triggered by Lipopolysaccharides. Plant Physiol **160**:1081–
- 896 1096
- 897
- 898 **Tada Y, Mori T, Shinogi T, Yao N, Takahashi S, Betsuyaku S, Sakamoto M, Park P, Nakayashiki H,**
- 899 **Tosa Y, and Mayama S** (2004) Nitric Oxide and reactive oxygen species do not elicit hypersensitive
- 900 cell death but induce apoptosis in the adjacent cells during the defense response of oat. Mol Plant
- 901 Microbe Interact **17**: 245-253
- 902
- 903 **Takai R, Isogai A, Takayama S, et al.** (2008) Analysis of flagellin perception mediated by Flg22
- 904 receptor OsFLS2 in rice. Molecular Plant-Microbe Interactions **21**: 1635-1642
- 905
- 906 **Takai R., Kaneda T, Isogai A, Takayama S, Che FS** (2007) A new method of defense response
- 907 analysis using a transient expression system in rice protoplasts. Biosci Biotechnol Biochem **71**: 590-593
- 908
- 909 **Thomma BP, Nurnberger T, Joosten MH** (2011) Of PAMPs and effectors: the blurred PTI-ETI
- 910 dichotomy. Plant Cell **23**: 4-15
- 911
- 912 **Thor K, Jiang S, Michard E, et al.** (2020) The calcium-permeable channel OSCA1.3 regulates plant
- 913 stomatal immunity. Nature **585**:569-573
- 914
- 915 **Vandelle E, Poinssot B, Wendehenne D, Bentejac M & Pugin A** (2006) Integrated signalling
- 916 network involving calcium, nitric oxide, and active oxygen species but not mitogen - activated protein

- 917 kinases in BcPG1-elicited grapevine defenses. *Mol Plant Microbe Interact* **19**: 429-440
918
- 919 **Wang S S, Zhao F Y, Wei X J, et al.** (2013) Preliminary study on Flg22-induced defense response in
920 female gametophytes in *Saccharina japonica* (Phaeophyta). *Journal of Applied Phycology* **25**: 1215-1223
921
- 922 **Wang XN** (2014) Study on the infection of cotton leaves and monocots by VD labeled with green
923 fluorescent protein. Nanjing Agricultural University
924
- 925 **Wang XY, Chen ZL, Liu WZ, et al.** (2015) Breeding of fla transgenic rice and analysis of disease
926 resistance spectrum. *Molecular Plant Breeding* **13**:61-65
927
- 928 **Wang XY, Chen ZY, Liu WZ, et al.** (2014) Resistance to Bacterial Leaf Streak of Transgenic Rice with
929 Flagellin Gene. *Acta Botanica Northwest* **34**:1534-1539
930
- 931 **Wang** (2012) A preliminary study on the defense response of kelp induced by Flg22. Ocean University
932 of China
933
- 934 **Yan J, Tsuchihara N, Etoh T, et al.** (2007) Reactive oxygen species and nitric oxide are involved in
935 ABA inhibition of stomatal opening. *Plant Cell Environ* **30**: 1320-1325
936
- 937 **Yano A, Suzuki K, Uchimiya H, Shinshi H** (1998) Induction of hypersensitive cell death by a fungal
938 protein in cultures of tobacco cells. *Mol Plant Microbe Interact* **11**: 115-123
939
- 940 **Yi SY, Kwon SY** (2014) How does SA signaling link the Flg22 responses? *Plant Signal Behav*
941 **9**:e972806
942
- 943 **Yi SY, Shirasu K, Moon JS, Lee SG, Kwon SY** (2014) The activated SA and JA signaling pathways
944 have an influence on flg22-triggered oxidative burst and callose deposition. *PLoS One* **9**:e88951
945
- 946 **Yuan P, Jewell JB, Behera S, Tanaka K, Poovaiah BW** (2020) Distinct Molecular Pattern-Induced
947 Calcium Signatures Lead to Different Downstream Transcriptional Regulations via AtSR1/CAMTA3. *Int*
948 *J Mol Sci* **21**:8163
949
- 950 **Zhang A, Jiang M, Zhang J, Ding H, Xu SH, Hu X** (2007) Nitric oxide induced by hydrogen peroxide

951 mediates abscisic acid-induced activation of mitogen-activated protein kinase cascade involved in
952 antioxidant defense in maize leaves. *New Phytol* **175**: 36-50

953

954 **Zipfel C, Robatzek S, Nacarro L, et al.** (2004) Bacterial disease resistance in Arabidopsis through
955 flagellin perception. *Nature* **428**: 764-767

956

957

958

959

960

961

962

963

964

965

966

967

968

969

970

971

972

973

974

975

976

977

978

979

980

Parsed Citations

Abeles FB, Forrence LE (1970) Temporal and hormonal control of beta-1, 3-glucanase in Phaseolus vulgaris L. Plant Physiol 45: 395–400

Google Scholar: [Author Only](#) [Title Only](#) [Author and Title](#)

Ali MB, Singh N, Shohael AM, et al. (2006) Phenolics metabolism and lignin synthesis in root suspension cultures of Panax ginseng in response to copper stress[J]. Plant Science 171: 147-154.

Google Scholar: [Author Only](#) [Title Only](#) [Author and Title](#)

Asai T, Tena G, Plotnikova J, et al. (2002) MAP kinase signaling cascade in Arabidopsis innate immunity. Nature 415: 977-983

Google Scholar: [Author Only](#) [Title Only](#) [Author and Title](#)

Besson-Bard A, Courtois C, Gauthier A, Dahan J, Dobrowolska G, Jeandroz S, Pugin A, Wendehenne D (2008) Nitric oxide in plants: production and cross-talk with Ca²⁺ signaling. Mol Plant 1:218-228

Bi G, Su M, Li N, Liang Y, Dang S, Xu J, Hu M, Wang J, Zou M, Deng Y, Li Q, Huang S, Li J, Chai J, He K, Chen YH, Zhou JM (2021) The ZAR1 resistosome is a calcium-permeable channel triggering plant immune signaling. Cell 184:3528-3541

Google Scholar: [Author Only](#) [Title Only](#) [Author and Title](#)

Bouizgarne B, El-Maarouf-Bouteau H, Frankart C, et al. (2006) Early physiological responses of Arabidopsis thaliana cells to fusaric acid: toxic and signalling effects. The New Phytologist 169: 209-218

Google Scholar: [Author Only](#) [Title Only](#) [Author and Title](#)

Brennan T, Frenkel C (1977) Involvement of hydrogen peroxide in the regulation of senescence in pear. Plant Physiol 59: 411–416

Google Scholar: [Author Only](#) [Title Only](#) [Author and Title](#)

Bright J, Desikan R, Hanecek J T, Weir S, Neill S J (2006) ABA induced NO generation and stomatal closure in Arabidopsis are dependent on H₂O₂ synthesis. The Plant J 45:113-122

Google Scholar: [Author Only](#) [Title Only](#) [Author and Title](#)

Buxdorf K, Rahat I, Gafni A, Levy M (2013) The epiphytic fungus Pseudozyma aphidis induces jasmonic acid- and salicylic acid/nonexpressor of PR1-independent local and systemic resistance. Plant Physiol 161:2014-2022

Google Scholar: [Author Only](#) [Title Only](#) [Author and Title](#)

Chen YL, Huang R, Xiao YM, Lü P, Chen J, Wang XC (2004) Extracellular calmodulin-induced stomatal closure is mediated by heterotrimeric G protein and H₂O₂. Plant Physiol 136: 4096–4103

Google Scholar: [Author Only](#) [Title Only](#) [Author and Title](#)

Daudi A, Cheng Z, O'Brien JA, Mammarella N, Khan S, Ausubel FM, Bolwell GP (2012) The apoplastic oxidative burst peroxidase in Arabidopsis is a major component of pattern-triggered immunity. Plant Cell 24:275-87

Google Scholar: [Author Only](#) [Title Only](#) [Author and Title](#)

Dickerson DP, Pascholati SF, Hagerman AE, Butler LG, Nicholson RL (1984) Phenylalanine ammonia-lyase and hydroxy cinnamate: CoA ligase in maize mesocotyls inoculated with Helminthosporium maydis or Helminthosporium carbonum. Physiol Plant Pathol 25: 111–123

Google Scholar: [Author Only](#) [Title Only](#) [Author and Title](#)

Dixon RA, Harrison MJ, and Lamb CJ (1994) Early events in the activation of plant defense responses. Annual Review of Phytopathology 32: 479-501

Google Scholar: [Author Only](#) [Title Only](#) [Author and Title](#)

Dong H, Li W, Zhang D, et al. (2003) Differential expression of induced resistance by an aqueous extract of killed Penicillium chrysogenum against Verticillium wilt of cotton[J]. Crop Protection 22: 129-134.

Google Scholar: [Author Only](#) [Title Only](#) [Author and Title](#)

Durrant WE, Dong X(2004) Systemic acquired resistance. Annual Review of Phytopathology 42: 185-209

Google Scholar: [Author Only](#) [Title Only](#) [Author and Title](#)

Ebel J, Mithöfer A(1998) Early events in the elicitation of plant defence. Planta 206: 335-348

Google Scholar: [Author Only](#) [Title Only](#) [Author and Title](#)

Emani C, Garcia JM, Lopata-Finch E, Pozo MJ, Uribe P, KimDJ, Sunilkumar G, Cook DR, Kenerley CM, Rathore KS (2003) Enhanced fungal resistance in transgenic cotton expressing an endochitinase gene from Trichoderma reesei. Plant Biotechnol J 1: 321–336

Google Scholar: [Author Only](#) [Title Only](#) [Author and Title](#)

Fan B, Shen L, Liu KL, et al. (2008) Interaction between nitric oxide and hydrogen peroxide in postharvest tomato resistance response to Rhizopus Nigricans. J Sci Food Agric 88: 1238-1244

Google Scholar: [Author Only](#) [Title Only](#) [Author and Title](#)

Felix G, Duran J D, Volko S, et al. (1999) Plants have a sensitive perception system for the most conserved domain of bacterial flagellin. Plant Journal 18: 265-276

Google Scholar: [Author Only](#) [Title Only](#) [Author and Title](#)

- Gómez-Gómez L, Boller T (2000) FLS2: an LRR receptor-like kinase involved in the perception of the bacterial elicitor flagellin in Arabidopsis. Molecular Cell 5: 1003-1011**
Google Scholar: [Author Only](#) [Title Only](#) [Author and Title](#)
- Han Q (2014) Screening and identification of cotton anti-VD biocontrol bacteria and research on disease resistance mechanism. Nanjing: Nanjing Agricultural University**
Google Scholar: [Author Only](#) [Title Only](#) [Author and Title](#)
- Holmes EC, Chen YC, Mudgett MB, Sattely ES. (2021) Arabidopsis UGT76B1 glycosylates N-hydroxy-pipecolic acid and inactivates systemic acquired resistance in tomato. Plant Cell 33:750-765**
Google Scholar: [Author Only](#) [Title Only](#) [Author and Title](#)
- Hu HL (2012) Construction of transgenic VD with GFP gene and study on the process of infecting cotton. Nanjing Agricultural University**
Google Scholar: [Author Only](#) [Title Only](#) [Author and Title](#)
- Jennings JC, Birkhold PC, Mock NM (2001) Induction of defense responses in tobacco by the protein Nep1 from Fusarium oxysporum. The Plant Science 161: 891-899**
Google Scholar: [Author Only](#) [Title Only](#) [Author and Title](#)
- Jones JD, Dangl JL (2006) The plant immune system. Nature 444: 323-329**
Google Scholar: [Author Only](#) [Title Only](#) [Author and Title](#)
- Kumar R, Barua P, Chakraborty N, Nandi AK (2020) Systemic acquired resistance specific proteome of Arabidopsis thaliana. Plant Cell Rep 39:1549-1563**
Google Scholar: [Author Only](#) [Title Only](#) [Author and Title](#)
- Kumar V, Parkhi V, Kenerley CM, et al. (2009) Defense-related gene expression and enzyme activities in transgenic cotton plants expressing an endochitinase gene from Trichoderma virens in response to interaction with Rhizoctonia solani. Planta 230: 277-291**
Google Scholar: [Author Only](#) [Title Only](#) [Author and Title](#)
- Lamotte O, Gould K, Lecourieux D, Sequeira-Legrand A, Lebrun -Garcia A, Durner J, Pugin A & Wende-henne D (2004) Analysis of nitric oxide signaling functions in tobacco cells challenged by the elicitor cryptogein . Plant Physiol 135: 516-529**
Google Scholar: [Author Only](#) [Title Only](#) [Author and Title](#)
- Li B, Fu Y, Jiang D, Xie J, Cheng J, Li G, Hamid MI, Yi X (2010) Cyclic GMP as a second messenger in the nitric oxide-mediated condiation of the mycoparasite Coniothyrium minitans. Appl Environ Microbiol 76: 2830–2836**
Google Scholar: [Author Only](#) [Title Only](#) [Author and Title](#)
- Liu P, Zhang H, Yu B, Xiong L, Xia Y (2015) Proteomic identification of early salicylate- and flg22-responsive redox-sensitive proteins in Arabidopsis. Sci Rep 27:8625**
Google Scholar: [Author Only](#) [Title Only](#) [Author and Title](#)
- Liu Q, Ding Y, Shi Y, Ma L, Wang Y, Song C, Wilkins KA, Davies JM, Knight H, Knight MR, Gong Z, Guo Y, Yang S (2021) The calcium transporter ANNEXIN1 mediates cold-induced calcium signaling and freezing tolerance in plants. EMBO J 40:e104559**
Google Scholar: [Author Only](#) [Title Only](#) [Author and Title](#)
- Livak KJ, Schmittgen TD (2001) Analysis of relative gene expression data using real-time quantitative PCR and the 2- $\Delta\Delta$ CT Method. Methods 25: 402–408**
Google Scholar: [Author Only](#) [Title Only](#) [Author and Title](#)
- Martínez-Medina A, Pescador L, Terrón-Camero LC, Pozo MJ, Romero-Puertas MC (2019) Nitric oxide in plant-fungal interactions. J Exp Bot 70:4489-4503**
Google Scholar: [Author Only](#) [Title Only](#) [Author and Title](#)
- Millet Y A, Danna C H, Clay N K, et al. (2010) Innate immune responses activated in Arabidopsis roots by microbe-associated molecular patterns. Plant Cell 22: 973-990**
Google Scholar: [Author Only](#) [Title Only](#) [Author and Title](#)
- Naveed ZA, Wei X, Chen J, Mubeen H, Ali GS (2020) The PTI to ETI Continuum in Phytophthora-Plant Interactions. Front Plant Sci 17: 593965**
Google Scholar: [Author Only](#) [Title Only](#) [Author and Title](#)
- Nicaise V, Roux M, Zipfel C (2009) Recent advances in PAMP-triggered immunity against bacteria: pattern recognition receptors watch over and raise the alarm. Plant Physiol 150: 1638-1647**
Google Scholar: [Author Only](#) [Title Only](#) [Author and Title](#)
- Nürnberg T, Brunner F (2002) Innate immunity in plants and animals: emerging parallels between the recognition of general elicitors and pathogen-associated molecular patterns. Current Opinion in Plant Biology 5: 318-324**
Google Scholar: [Author Only](#) [Title Only](#) [Author and Title](#)
- Plazek A, Zur I (2003) Cold-induced plant resistance to necrotrophic pathogens and antioxidant enzyme activities and cell membrane permeability. Plant Sci 164: 1019–1028**
Google Scholar: [Author Only](#) [Title Only](#) [Author and Title](#)

- Pomar F, Merino F, Barceló AR (2002) O-4-Linked coniferyl and sinapyl aldehydes in lignifying cell walls are the main targets of the Wiesner (phloroglucinol-HCl) reaction. *Protoplasma* 220: 17-28
Google Scholar: [Author Only](#) [Title Only](#) [Author and Title](#)
- Qiao M, Sun J, Liu N, Sun T, Liu G, Han S, Hou C, Wang D (2015) Changes of Nitric Oxide and Its Relationship with H₂O₂ and Ca²⁺ in Defense Interactions between Wheat and *Puccinia Triticina*. *PLoS One* 10:e0132265
Google Scholar: [Author Only](#) [Title Only](#) [Author and Title](#)
- Ren A, Li MJ, Shi L, Mu DS, Jiang AL, Han Q, Zhao MW (2013) Profiling and quantifying differential gene transcription provide insights into ganoderic acid biosynthesis in *Ganoderma lucidum* in response to methyl jasmonate. *PLoS One* 8: e65027
Google Scholar: [Author Only](#) [Title Only](#) [Author and Title](#)
- Richard Hilleary, Julio Paez-Valencia, Cullen Vens, Masatsugu Toyota, Simon Gilroy (2020) Tonoplast-localized Ca²⁺ pumps regulate Ca²⁺ signals during pattern-triggered immunity in *Arabidopsis thaliana*. *Proceedings of the National Academy of Sciences* 117:18849-18857
Google Scholar: [Author Only](#) [Title Only](#) [Author and Title](#)
- Sang J, Jiang M, Lin F, et al. (2008) Nitric oxide reduces hydrogen peroxide accumulation involved in water stress-induced subcellular antioxidant defense in maize plants. *J Integr Plant Biol* 50: 231-243
Google Scholar: [Author Only](#) [Title Only](#) [Author and Title](#)
- Sudhakar C, Lakshmi A, Giridarakumar S (2001) Changes in the antioxidant enzyme efficacy in two high yielding. *Plant Sci* 161: 613– 619
Google Scholar: [Author Only](#) [Title Only](#) [Author and Title](#)
- Sun A, Nie S, Xing D (2012) Nitric oxide-mediated maintenance of redox homeostasis contributes to NPR1-dependent plant innate immunity triggered by Lipopolysaccharides. *Plant Physiol* 160:1081–1096
Google Scholar: [Author Only](#) [Title Only](#) [Author and Title](#)
- TadaY, Mori T, Shinogi T, Yao N, Takahashi S, Betsuyaku S, Sakamoto M, Park P, Nakayashiki H, Tosa Y, and Mayama S (2004) Nitric Oxide and reactive oxygen species do not elicit hypersensitive cell death but induce apoptosis in the adjacent cells during the defense response of oat. *Mol Plant Microbe Interact* 17: 245-253
Google Scholar: [Author Only](#) [Title Only](#) [Author and Title](#)
- Takai R, Isogai A, Takayama S, et al. (2008) Analysis of flagellin perception mediated by Flg22 receptor OsFLS2 in rice. *Molecular Plant-Microbe Interactions* 21: 1635-1642
Google Scholar: [Author Only](#) [Title Only](#) [Author and Title](#)
- Takai R., Kaneda T, Isogai A, Takayama S, Che FS (2007) A new method of defense response analysis using a transient expression system in rice protoplasts. *Biosci Biotechnol Biochem* 71: 590-593
Google Scholar: [Author Only](#) [Title Only](#) [Author and Title](#)
- Thomma BP, Nurnberger T, Joosten MH (2011) Of PAMPs and effectors: the blurred PTI-ETI dichotomy. *Plant Cell* 23: 4-15
Google Scholar: [Author Only](#) [Title Only](#) [Author and Title](#)
- Thor K, Jiang S, Michard E, et al. (2020) The calcium-permeable channel OSCA1.3 regulates plant stomatal immunity. *Nature* 585:569-573
Google Scholar: [Author Only](#) [Title Only](#) [Author and Title](#)
- Vandelle E, Poinssot B, Wendehenne D, Bentejac M & Pugin A (2006) Integrated signalling network involving calcium, nitric oxide, and active oxygen species but not mitogen - activated protein kinases in BcPG1-elicited grapevine defenses. *Mol Plant Microbe Interact* 19: 429-440
Google Scholar: [Author Only](#) [Title Only](#) [Author and Title](#)
- Wang S S, Zhao F Y, Wei X J, et al. (2013) Preliminary study on Flg22-induced defense response in female gametophytes in *Saccharina japonica* (Phaeophyta). *Journal of Applied Phycology* 25: 1215-1223
Google Scholar: [Author Only](#) [Title Only](#) [Author and Title](#)
- Wang XN (2014) Study on the infection of cotton leaves and monocots by VD labeled with green fluorescent protein. Nanjing Agricultural University
Google Scholar: [Author Only](#) [Title Only](#) [Author and Title](#)
- Wang XY, Chen ZL, Liu WZ, et al. (2015) Breeding of fla transgenic rice and analysis of disease resistance spectrum. *Molecular Plant Breeding* 13:61-65
Google Scholar: [Author Only](#) [Title Only](#) [Author and Title](#)
- Wang XY, Chen ZY, Liu WZ, et al. (2014) Resistance to Bacterial Leaf Streak of Transgenic Rice with Flagellin Gene. *Acta Botanica Northwest* 34:1534-1539
Google Scholar: [Author Only](#) [Title Only](#) [Author and Title](#)
- Wang (2012) A preliminary study on the defense response of kelp induced by Flg22. Ocean University of China
Google Scholar: [Author Only](#) [Title Only](#) [Author and Title](#)
- Yan J, Tsuchihara N, Etoh T, et al. (2007) Reactive oxygen species and nitric oxide are involved in ABA inhibition of stomatal opening. *Plant Cell Environ* 30: 1320-1325

Google Scholar: [Author Only](#) [Title Only](#) [Author and Title](#)

Yano A, Suzuki K, Uchimiya H, Shinshi H (1998) Induction of hypersensitive cell death by a fungal protein in cultures of tobacco cells. Mol Plant Microbe Interact 11: 115-123

Google Scholar: [Author Only](#) [Title Only](#) [Author and Title](#)

Yi SY, Kwon SY (2014) How does SA signaling link the Flg22 responses? Plant Signal Behav 9:e972806

Yi SY, Shirasu K, Moon JS, Lee SG, Kwon SY (2014) The activated SA and JA signaling pathways have an influence on flg22-triggered oxidative burst and callose deposition. PLoS One 9:e88951

Google Scholar: [Author Only](#) [Title Only](#) [Author and Title](#)

Yuan P, Jewell JB, Behera S, Tanaka K, Poovaiah BW (2020) Distinct Molecular Pattern-Induced Calcium Signatures Lead to Different Downstream Transcriptional Regulations via AtSR1/CAMTA3. Int J Mol Sci 21:8163

Google Scholar: [Author Only](#) [Title Only](#) [Author and Title](#)

Zhang A, Jiang M, Zhang J, Ding H, Xu SH, Hu X (2007) Nitric oxide induced by hydrogen peroxide mediates abscisic acid-induced activation of mitogen-activated protein kinase cascade involved in antioxidant defense in maize leaves. New Phytol 175: 36-50

Google Scholar: [Author Only](#) [Title Only](#) [Author and Title](#)

Zipfel C, Robatzek S, Nacarro L, et al. (2004) Bacterial disease resistance in Arabidopsis through flagellin perception. Nature 428: 764-767

Google Scholar: [Author Only](#) [Title Only](#) [Author and Title](#)